



**score**



This project has received funding from the European Union's Horizon 2020 research and innovation programme under grant agreement No 101003534



## DOCUMENT TRACKS DETAILS

Project acronym	SCORE
Project title	Smart Control of Climate Resilience in European Coastal Cities
Starting date	01.07.2021
Duration	48 months
Call identifier	H2020-LC-CLA-2020-2
Grant Agreement No	101003534

Deliverable Information	
Deliverable number	D3.8
Work package number	WP3 - Regional and Local Projections, Analyses, Modelling and Uncertainties
Deliverable title	Short-term hazard modelling
Lead beneficiary	SAMU & LAMMA
Author(s)	Neslihan Beden, Vahdettin Demir, Nazire Göksu Soydan Oksal, Sema Arıman, Şule Haliloğlu, Bahtiyar Efe (SAMU); Carlo Brandini, Alberto Ortolani, Michele Bondoni, Rossella Mocali (LAMMA)
Due date	30/06/2024
Actual submission date	30/06/2024
Type of deliverable	Report
Dissemination level	Public

## VERSION MANAGEMENT

Revision table			
Version	Name	Date	Description
V 0.1	Neslihan Beden, Vahdettin Demir, Nazire Göksu Soydan Oksal, Sema Arıman, Şule Haliloğlu, Bahtiyar Efe (SAMU)	15/06/2024	First draft
V 0.2	Michele Bondoni, Rossella Mocali (LAMMA)	20/06/2024	Second Draft
V 0.3	Carlo Brandini (LAMMA)	23/06/2024	Document review





V 0.3	Luis Angel Espinosa Villalpando, Cecil Meulenberg, Jacek Baranzcuk	27/06/2024	Document review
V 0.3	Neslihan Beden, Nazire Göksu Soydan Oksal, Vahdettin Demir, Şule Haliloğlu (SAMU)	28/06/2024	Document review
V 0.3	Neslihan Beden (SAMU)	29/06/2024	Third Draft
V1.0	Neslihan Beden (SAMU), Rossella Mocali, Carlo Brandini (LaMMA), Salem Gharbia	30/06/2024	Final version

All information in this document only reflects the author's point of view. The European Commission is not responsible for any use that may be made of the information it contains.

## LIST OF ACRONYMS AND ABBREVIATIONS

Acronym / Abbreviation	Meaning / Full text
EBAs	Ecosystem-Based Approaches
CCLL	Coastal City Living Lab
RPO	Research Performing Organisation
SME	Small and Medium Sized Enterprise
WP	Work Package
HEC-RAS	Hydrologic Engineering Center's River Analysis System
SW	Software
RCP	Representative Concentration Pathways
IPCC	Intergovernmental Panel on Climate Change
RCD	Regional Climate Downscaling
WCRP	The World Climate Research Programme
CORDEX	Coordinated Regional Downscaling Experiment
RCM	Regional Climate Model
SLR	Sea Level Rise
DEM	Digital Elevation Model
DTM	Digital Terrain Model





DT	Digital Twin
n	Manning roughness coefficient
2D	One dimensional
1D	Two dimensional
ED50	European Datum 1950
UTM	Universal Transverse Mercator
CORINE	Coordination of Information on the Environment
EWSS	Early Warning Support System





## BACKGROUND: ABOUT THE SCORE PROJECT

The intensification of extreme weather events, coastal erosion, and sea-level rise are significant challenges to be urgently addressed by European coastal cities. The science behind these disruptive phenomena is complex, and advancing climate resilience requires progress in data acquisition, forecasting, and understanding the potential risks and impacts of real-scenario interventions. The Ecosystem-Based Approach (EBA) supported by smart technologies has the potential to increase the climate resilience of European coastal cities; however, it still needs to be adequately understood and coordinated at European level.

SCORE is a four-year EU-funded project aiming to increase climate resilience in European coastal cities. The SCORE project outlines a co-creation strategy, developed via a network of 10 coastal city 'living labs' (CCLLs), to rapidly, equitably, and sustainably enhance coastal city climate resilience through EBAs and sophisticated digital technologies.

The 10 coastal city living labs involved in the project are Sligo and Dublin, Ireland; Barcelona/Vilanova I la Geltrú, Benidorm and Basque Country, Spain; Oeiras, Portugal; Massa, Italy; Piran, Slovenia; Gdansk, Poland; and Samsun, Turkiye.

SCORE will establish an integrated coastal zone management framework for strengthening EBA and smart coastal city policies, creating European leadership in coastal city climate change adaptation in line with The Paris Agreement. It will provide innovative platforms to empower stakeholders' deployment of EBAs to increase climate resilience, business opportunities, and financial sustainability of coastal cities.

The SCORE interdisciplinary team consists of 28 world-leading organizations from academia, local authorities, RPOs, and SMEs, encompassing a wide range of skills, including environmental science and policy, climate modelling, citizen and social science, data management, coastal management and engineering, security and technological aspects of smart sensing research.





## EXECUTIVE SUMMARY

This document is a deliverable of the SCORE project, funded under the European Union's Horizon 2020 research and innovation program under grant agreement No 101003534.

This document describes the processing tools and data of D3.7 (<https://doi.org/10.5281/zenodo.10417524>). It includes a brief theoretical explanation of the short-term hazard modelling tools, a description of their usage, and the modelling results of the frontrunner cities: Samsun, Massa, Villanova, and Oarsoaldea.

## LINKS WITH OTHER PROJECT ACTIVITIES

The D3.8, related to Task 3.4 and entitled "Short-term hazard modelling" is the eighth WP3 report. This report addresses the "last mile" hydraulic models, which take as input the climatic information produced by the hydrological downscaling models, sea level models, and wave models, resulting from Task 3.2 and described in deliverables D3.3 and D3.4. These models are used on an urban scale, considering digital terrain models and all the very precise and detailed information at these scales. Such scenarios are built to take into account the main hazard situations with different occurrence probabilities and are determined on the basis of the statistical tools defined in Task 3.3.

The results produced by the models in this role are crucial for risk estimation in WP6 and related Ecosystem-Based Approaches (EBAs) adaptation strategies in WP7. The outputs of this Task 3.4 will be finally tested through a general analysis procedure in Task 3.6. The outputs produced in this task are among the primary sources of data generation for the entire project, stored in the SCORE ICT Platform (SIP) (WP5). Furthermore, elaborated by state-of-the-art models, they accompany the results of the Digital Twin (DT) and EWSS (Early Warning Support System) models (WP8), compared to which they are used for comparison and validation of results.





## TABLE OF CONTENT

1. Introduction	9
1.1 Scope of the deliverable	9
1.3. Structure and content of the deliverable	9
2. HYDRAULIC MODELLING AT URBAN SCALE	9
2.3. Land flood modelling	10
2.4. Coastal flood modelling	11
2.2.1. XBeach	11
2.2.2. Simplified approach	12
3. STUDY CASES AND RESULTS	13
3.1. Samsun CCLL	13
3.1.1. Meteorological data	16
3.1.2. Future Scenarios - RCP 4.5 and RCP 8.5	17
3.1.3. CORDEX	18
3.1.4. Hydrological modelling	18
3.1.5. Hydraulic modelling results	21
3.1.5.1. Land flooding results	21
3.1.5.2. Coastal flooding results	22
3.2 Massa	25
3.3 Vilanova i la Geltrú	25
3.4 Oarsoaldea	25
4. Conclusions and recommendation	25
5. References	26





## INDEX OF FIGURES

Figure 1. Manning “n” values of Samsun CCLL.	14
Figure 2. The base flow time-sequential flow chart.	14
Figure 3. Flow chart of hydraulic modelling.	16
Figure 4. Schematic representation of the main hazards identified for the ten CCLLs (Rebollido and Iglesias, 2023).	20
Figure 5. Samsun CCLL and its land cover (Rebollido and Iglesias, 2023).	20
Figure 6. Kızılırmak Basin and Bafra Plain.	21
Figure 7. DEM of the flood model area.	22
Figure 8. Thiessen polygons and meteorological station location.	23
Figure 9. Monthly precipitation and temperatures over 1976 and 2022 as recorded in the Bafra station.	23
Figure 10. Flow chart of hydrological modelling.	26
Figure 11. River cross sections and 1D modelling.	27
Figure 12. Flood hydrographs for different return periods.	28
Figure 13. Flood propagation and water velocity maps for different periods (historical land flood modelling).	30
Figure 14. Flood propagation and water velocity maps for different periods (RCP 4.5).	30
Figure 15. Flood propagation and water velocity maps for different periods (RCP 8.5).	30
Figure 16. Bathymetry input and grid structure for Xbeach model.	32
Figure 17. Coastal flood modelling water level and wave height results.	33
Figure 18. Coupled land and coastal flood modelling results.	34
Figure 19. Massa CCLL.	35
Figure 20. Study area in HEC-RAS with DEM and 1D Frigido river.	35
Figure 21. Example of a river cross section in 1D modelling.	35
Figure 22. Example of a bridge modelling.	36
Figure 23. 2D flow area mesh, lateral structures, cross sections.	36
Figure 24. Hazard maps for river flood, return periods 5, 25, 50, 100, 200, 500 years, Historical 1956-2005.	38
Figure 25. Hazard maps for river flood, return period 200 years, RCP 4.5.	38
Figure 26. Hazard maps for river flood, return period 200 years, RCP 8.5.	38
Figure 27. Hazard maps for coastal flood, return period 500 years, Historical, RCP 4.5, RCP 8.5.	39
Figure 28. Hazard maps for river flood, return period 200 years, RCP 4.5 without and with riparian reforestation.	40
Figure 29. Urbanized area along river Frigido.	41
Figure 30. River Frigido profile – baseline and riverbed excavation.	41
Figure 31. Hazard maps for river flood, return period 100 years, RCP 8.5 without and with EBA implementation.	41
Figure 32. Vilanova i la Geltrú CCLL.	42
Figure 33. Study area in HEC-RAS.	43
Figure 34. Focus area in hazard maps.	44
Figure 35. Hazard maps for river flood, return periods 5, 25, 50, 100, 200, 500 years, Historical 1956-2005.	45
Figure 36. Hazard maps for river flood, return period 200 years, RCP 4.5.	45
Figure 37. Hazard maps for river flood, return period 200 years, RCP 8.5.	46
Figure 38. Hazard maps for coastal flood, return period 500 years, Historical, RCP4.5, RCP 8.5	47
Figure 39. Wall between the beach and the street.	47
Figure 40. River bank elevation before and after EBA implementation – Cross section 40.	48
Figure 41. River bank elevation before and after EBA implementation – Cross section 33.	48
Figure 42. River bank elevation before and after EBA implementation – Cross section 18.	49
Figure 43. Hazard maps for river flood, return period 25 years, RCP 4.5 without (left) and with EBA implementation (right).	49
Figure 44. Hazard maps for river flood, return period 100 years, RCP 8.5 without (left) and with EBA implementation (right).	49
Figure 45. Oarsoaldea CCLL.	50
Figure 46. A 1D/2D hydraulic model on HEC-RAS was implemented, where both rivers have a 1D structure.	51





## INDEX OF TABLES

<i>Table 1. CORINE classes and Manning n coefficients of these classes.</i>	12
<i>Table 2. Raw data needed to create the geometry and input files.</i>	14
<i>Table 3. Input files to launch a simulation.</i>	14
<i>Table 4. Input files to launch a simulation.</i>	16
<i>Table 5. Descriptive statistical information about precipitation and temperature data.</i>	21
<i>Table 6. Details of the CORDEX precipitation data for Turkiye.</i>	23
<i>Table 7. Return periods of 1D modelling.</i>	25
<i>Table 8. Summary of hydrological modelling results.</i>	27
<i>Table 9. Summary of flooded areas and average speeds.</i>	30





# 1 INTRODUCTION

## 1.1 Scope of the deliverable

As with the rest of the world, the impact of climate change on coastal cities has increased recently. Coastal cities are more affected by climate change and face natural hazards due to their geographical structure and topology. The SCORE project aims to acquire and share knowledge and experiences to mitigate the effects of extreme events in European coastal cities resulting from climate change. SCORE also seeks to enhance understanding and improve responses to various extreme natural hazards impacting these cities.

This deliverable aims to technically describe the tools and procedures (outlined in D3.7, including software scripts and data files) for short-term hazard models. The objective is to utilize the data provided by specific downscaling procedures—when deemed applicable—and the related historical series produced as climate projections within short-term models (i.e., on the scale of individual flood events). These procedures will be applied to different case studies and datasets, serving as examples during implementation.

A comprehensive data definition and collection study was carried out to perform short-term flood modelling and determine how much area would be damaged by floods. Short-term flood modelling was carried out in the frontrunner cities of WP3, Samsun, Massa, Villanova and Oarsoaldea, within the scope of the SCORE project. Part of the data is already available online, and the links are provided in the D3.7. However, some of the data received (subject to special permission) have been used for the project and are available in the specific script folder associated with the present document. The short-term hazard modelling is used to calculate the distribution areas and water heights of floods that may occur on land and on the coast and to determine the areas at risk. The main output of this report is to determine how much area is affected by land and coastal floods resulting concurrently from extreme meteorological conditions derived from climate scenarios, including sea level rise in coastal cities. High-level/reference maps produced by short-term flood modelling are provided, showing areas and water levels that may be affected by floods.

It is expected that the results of the aforementioned studies will be further validated within Task 3.6, and their accuracy and relevance in the adaptation process to climate change will be assessed. At the same time, these results aim to serve as a useful tool for the SCORE project objectives.

## 1.2 Structure and content of the deliverable

The deliverable is organized in several sections related to short term hazard modelling. Each section provides a short introductory description of the content and a table listing and addressing the different SW tools (models, scripts, data files, etc.). A folder is associated with this deliverable organized in





subfolders mapping the different sections and containing the tools developed for the project (and not available on other web repositories).

## 2 HYDRAULIC MODELLING AT URBAN SCALE

Hydraulic simulations are built on the climate projections and evaluate the dynamic contributions of hydrological floods and sea level dynamics (storm surge, tides) including the wave-induced sea levels (wave set-up and wave run up). Flood models conducted by using the one-dimensional (1D) and two-dimensional (2D) hydraulic model software from the United States Army Corps of Engineers, HEC-RAS (USACE, 2018).

Flooding will be exacerbated by potentially destructive storm surge impacts in coastal regions, where changes to beaches are evaluated using XBeach coastal wave models that incorporate a movable seabed, employing both a 2D phase-resolving and simplified approach.

### 2.1 Land flood modelling

Numerical modelling of overland floods was carried out with HEC-RAS. HEC-RAS is designed to perform 1D and 2D hydraulic calculations for a full network of natural and constructed channels (Brunner, G. W., 2016). The HEC-RAS executable code and documentation are public domain software which have been developed by the Hydrological Engineering Center for the U. S. Army Corps of Engineer's (USACE). This software can be downloaded for free. Initial data required for land flood modelling by HEC-RAS are the digital elevation model with a defined coordinate system, sections along the river or channel, geometric features of water structures on the river, structural layers or digital terrain model, flood hydrographs in various return periods, base flow value, river profile slope information, maps of the study area or satellite images, some map layers in the digital environment (roads, buildings, green areas, schools, etc.), Manning n roughness coefficient, and boundary conditions are required.

In the HEC-RAS model, a 1D energy equation solution is used as a simple computational method (Equation 1).

$$Z_2 + Y_2 + a_2 V_2^2 = \frac{Z_1}{2g} + Y_1 + a_2 V_1^2 + \frac{h_e}{2g} \quad (1)$$

$Z_1, Z_2$  main channel elevation inverted (m);  $Y_1, Y_2$  cross-sectional water depth (m);  $V_1, V_2$  average velocities (total release/total flow area);  $a_1, a_2$  coefficients for the velocity weighting;  $g$  acceleration of gravity; and  $h_e$  is the loss head of energy (m) which is determined by the Manning formula.

Users of the 2D HEC-RAS model can choose from three equation sets: 2D diffusion wave equations (Equation 2-4), shallow water equations, which use the Eulerian–Lagrangian approach to solve for advection, or a new shallow water equations solver, which uses a Eulerian approach. The basis for the shallow water equations are the Navier–Stokes equations, which are equations of conservation of mass and conservation of linear momentum, which continue to remain true under assumptions of shallow water breakdown, such as across a hydraulic jump. The shallow water equations are as follows for a horizontal bed with negligible Coriolis forces, frictional forces, and viscous forces (Peker et al., 2024),





$$\frac{\partial(\rho\eta)}{\partial t} + \frac{\partial(\rho\eta u)}{\partial x} + \frac{\partial(\rho\eta v)}{\partial y} = 0 \quad (2)$$

$$\frac{\partial(\rho\eta u)}{\partial t} + \frac{\partial}{\partial x}(\rho\eta^2 \rho g \eta^2) + \frac{1}{2} \frac{\partial(\rho\eta uv)}{\partial y} = 0 \quad (3)$$

$$\frac{\partial(\rho\eta v)}{\partial t} + \frac{\partial(\rho\eta uv)}{\partial x} + \frac{\partial}{\partial y}(\rho\eta v^2 + \frac{1}{2} \rho g \eta^2) = 0 \quad (4)$$

The “ $\eta$ ” symbol here represents the total fluid column height (the instantaneous fluid depth as a function of  $x$ ,  $y$ , and  $t$  and the 2D vector  $(u, v)$  represents the fluid’s average horizontal flow velocity across the vertical column. Further,  $g$  stands for gravitational acceleration and  $\rho$  for fluid density (USACE, 2018)

The first stage of Land flood modelling with HEC-RAS includes high-resolution DEM data. For SCORE’s test land-flood model the province of Samsun was used, and the data was obtained from the Turkish General Directorate of Mapping. The DEM data used in this study has a resolution of 5 meters and was obtained using remote sensing techniques. In hydraulic modelling, the DEM was clipped including the Bafra province of Samsun, which is the urban region in the basin, and the application area boundaries were determined. Before designing a land flood model, it is recommended the creation of a projection. This can be accomplished by using a projection file named “.prj”. The Set Projection option enables users to define the project’s spatial reference system. For example, the defined information for Samsun CCLL is “*ED50 / UTM zone 36N*”. In the second stage, the calculation mesh dimensions were selected as 5 meters to be compatible with the DEM. In the Land flood modelling as surface Manning “ $n$ ” values were determined using CORINE data from 2018 and the coefficients defined for these surfaces in the literature (Papaioannou, 2018). Table 1 includes CORINE classes and Manning  $n$  coefficients of these classes. In addition, the change in Manning  $n$  values of the study area is shown in Figure 1.

Table 1. CORINE classes and Manning  $n$  coefficients of these classes.





<b>Corine land cover classes and Manning's roughness coefficient</b>					
<b>1. Artificial surfaces</b>		Mannings n	<b>3. Forest and semi natural areas</b>		Mannings n
1.1 Urban Fabric			3.1 Forests		
	1.1.1. Continuous urban fabric	0.013		3.1.1. Broad-leaved forest	0.1
	1.1.2. Discontinuous urban fabric	0.013		3.1.2. Coniferous forest	0.1
1.2 Industrial, commercial and transport units				3.1.3. Mixed forest	0.1
	1.2.1. Industrial or commercial units	0.013	3.2 Scrub and/or herbaceous vegetation associations		
	1.2.2. Road and rail networks and associated land	0.013		3.2.1. Natural grasslands	0.04
	1.2.3. Port areas	0.013		3.2.2. Moors and heathland	0.05
	1.2.4. Airports	0.013		3.2.3. Sclerophyllous vegetation	0.05
1.3 Mine, dump and construction site				3.2.4. Transitional woodland-shrub	0.06
	1.3.1. Mineral extraction sites	0.013	3.3 Open spaces with little or no vegetation		
	1.3.2. Dump sites	0.013		3.3.1. Beaches, dunes, sands	0.025
	1.3.3. Construction sites	0.013		3.3.2. Bare rocks	0.035
1.4 Artificial, non-agricultural vegetated areas				3.3.3. Sparsely vegetated areas	0.027
	1.4.1. Green urban areas	0.025		3.3.4. Burnt areas	0.025
	1.4.2. Sport and leisure facilities	0.025		3.3.5. Glaciers and perpetual snow	0.01
<b>2. Agricultural areas</b>			<b>4. Wetlands</b>		
2.1 Arable land			4.1 Inland wetlands		
	2.1.1. Non-irrigated arable land	0.03		4.1.1. Inland marshes	0.04
	2.1.2. Permanently irrigated land	0.03		4.1.2. Peat bogs	0.04
	2.1.3. Rice fields	0.03	4.2 Coastal wetlands		
2.2 Permanent crops				4.1.1. Salt marshes	0.04
	2.2.1. Vineyards	0.08		4.1.2. Salines	0.04
	2.2.2. Fruit trees and berry plantations	0.08		4.2.3. Intertidal flats	0.04
	2.2.1. Olive groves	0.08	<b>5. Water bodies</b>		
2.3 Pastures			5.1 Inland waters		
	2.3.1. Pastures	0.035		5.1.1. Water courses	0.05
2.4. Heterogeneous agricultural areas				5.1.2. Water bodies	0.05
	2.4.1. Annual crops associated with permanent crops	0.04	5.2 Marine waters		
	2.4.2. Complex cultivation patterns	0.04		5.2.1. Coastal lagoons	0.07
	2.4.3. Land principally occupied by agriculture	0.05		5.2.1. Estuaries	0.07
	2.4.4. Agro-forestry areas	0.06		5.2.3. Sea and ocean	0.07



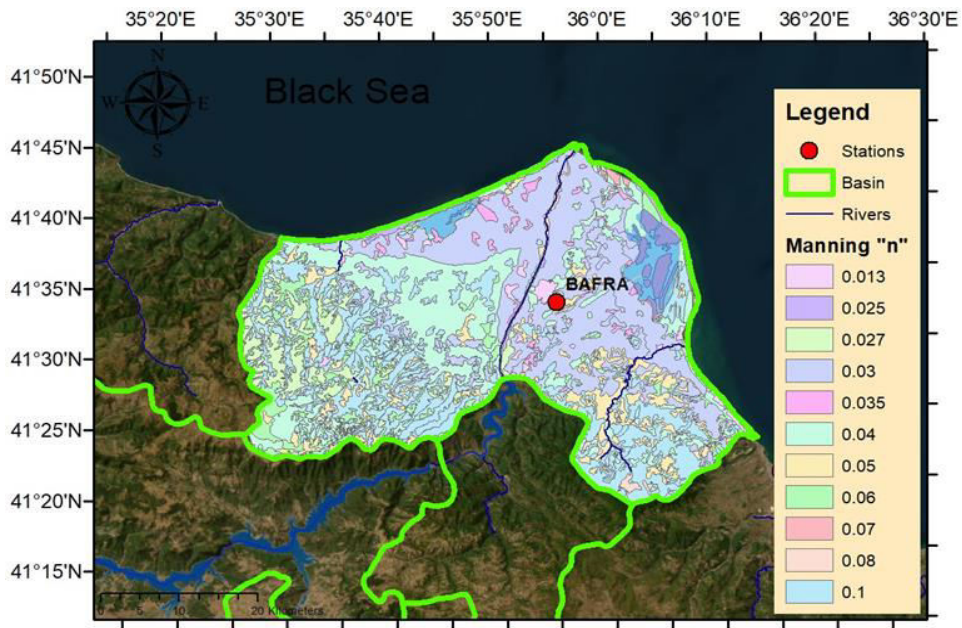


Figure 1. Manning “n” values of Samsun CCLL.

The base flow was determined using data from the Derbent station D15A318 in Bafra. The base flow was taken as the flow that occurred 95% of the time after visualizing the flow-time curves of the monthly average flows of the river. Artificial sequential flow data was obtained with the help of the Equation 5 below.

$$\dot{g} = \frac{m}{N + 1} \quad (5)$$

Here,  $m$  is the rank value and  $N$  is the number of data. The plot of change in percentage of time for artificial sequential data is shown in Figure 2.

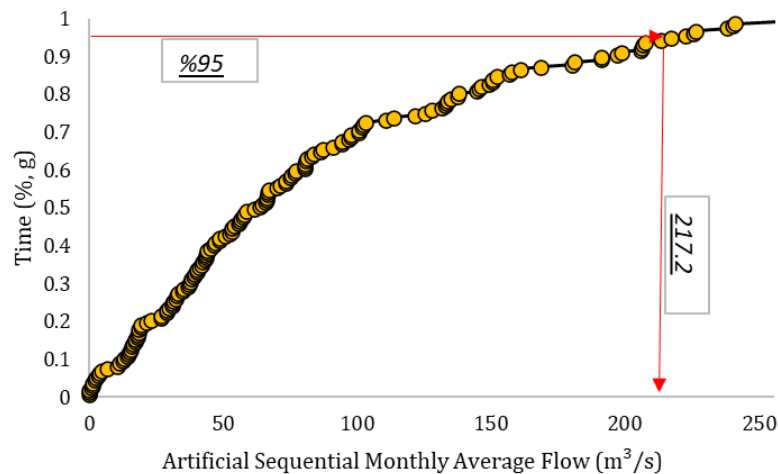


Figure 2. The base flow time-sequential flow chart.

In Figure 2, the current flow rate was read 95% of the time and was determined to be 217.2 m<sup>3</sup>/s. This obtained base flow value was added as a constant throughout of the hydrographs consisting of surface flow calculated by the synthetic unit hydrograph methods (Şen, 2009).



For Samsun CCLL, 1D modelling, steady modelling flow rates were obtained using annual instantaneous maximum flows and statistical methods. Unsteady flow data (2D) was obtained from the probability distributions of instantaneous maximum precipitation and the rainfall–runoff relationship was obtained using the DSI synthetic method (which is considered appropriate for the region). Then, the river slope was determined in the GIS environment (0.001) and the model was run with the boundary conditions defined as the inflow hydrograph and normal depth. Figure 3 shows the flow chart of HEC-RAS modelling. Table 2 contains the data needed to elaborate in order to create the input files to run the model, whereas Table 3 contains the input files to launch a simulation.

Table 2. Raw data needed to create the geometry and input files.

<b>Needed data to run the model</b>	<b>What</b>	<b>Description</b>
	DEM	Digital elevation model of the geographical domain, containing information about the buildings
	River data	Dataset containing river path coordinates and cross sections
	Hydraulic structures	Data related to the presence of hydraulic structures within the river bed or at the coast
	Bathymetry	Elevation of the underwater coastal area
	Discharge	Time series of discharge to be imposed to the upstream boundary
	Water level	Time series of water level to be imposed at coast, close to the shoreline

Table 3. Input files to launch a simulation.

<b>Needed files to run the model</b>	<b>Name</b>	<b>Description</b>
	modelName.prj	Project file
	modelName.pXX	File associated to a specific plan
	modelName.gYY	File associated to a specific geometry
	modelName.uZZ	File associated to specific boundary conditions



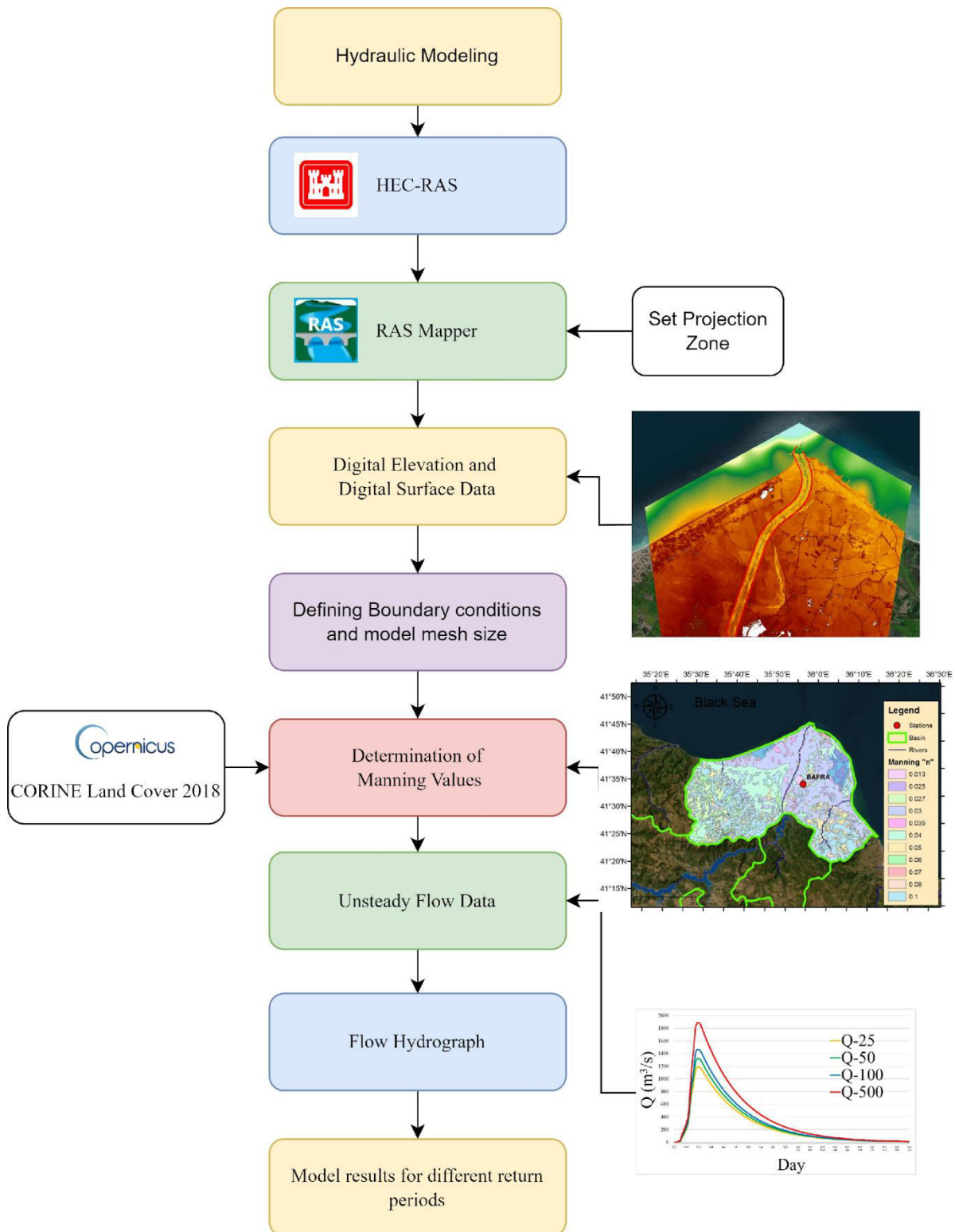


Figure 3. Flow chart of hydraulic modelling.

## 2.2 Coastal flood modelling

### 2.2.1 XBeach

XBeach is a nonlinear shallow water model for infragravity waves and a coupled stochastic (phase-



averaged) spectral wave model for storm-induced waves (Roelvink et al. 2009). The model is used for the computation of nearshore hydrodynamics and the morphodynamic response during storm events, such as dune erosion, overwash, and scouring around buildings. XBeach features a hydrodynamic model simulating mean currents in combination with a wave action conservation equation and an embedded sediment transport and morphodynamic model, which describes storm-induced changes in coastal sea bed level.

The description of the numerical model, its application to a study site, and the adopted simulation setup is reported in this deliverable. This document provides a comprehensive guide for conducting coastal modelling using the XBeach model with a discharge input. The steps outlined include the preparation of input data, model setup, execution, and analysis of results. The necessary input data for the XBeach model are given in Table 4.

Table 4. Input files to launch a simulation.

	Name	Description
Necessary files to run the model	params.txt	Parameters input file
	modelname.dep	Bathymetry file
	modelname.grd	Grid file
	zs0file	Offshore water level
	bcfile	Offshore wave climate file

To set up the XBeach model, one should start by obtaining the Digital Elevation Model (DEM) data for the coastal region of interest. Ensure that the DEM data is in a format compatible with XBeach, such as ASCII grid or netCDF. The next step is using a GIS tool or scripting to generate a regular grid that covers the coastal zone and river inlets. After the generation of grid cells, the bathymetric data for the model domain should be incorporated into a file named `modelname.dep`. Then, the model parameters are defined in the `params.txt` file. Key parameters of this file include the number of grid cells (nx, ny), grid cell size (dx, dy), simulation end time (tstop), and time step (dt). Documentation of the wave boundary conditions, which include significant wave height, wave period, and direction is the next step of preparation of input data for Xbeach. Finally, the user specifies the offshore water level. After simulating the water level with the Xbeach model, the water level output in the land boundary is used in land flood model (HEC-RAS) for coupling of the two models.

### 2.2.2 Simplified approach

The employ of the XBeach model can be quite demanding, even for 1D simulations over multiple cross sections, in case several runs need to be performed. Furthermore, both the water level and the wave spectrum need to be imposed as boundary conditions. In case a storm surge event associated to a specific





return period is simulated, it is necessary to perform a multivariate extreme value analysis of water level and wave height. Indeed, the probability of a compound event can be simply calculated by the product of the probability associated to the single events only if those events are independent. However, water level and wave height are generally correlated. To speed up the procedure, a simplified approach is proposed where the use of the XBeach model is avoided and the multivariate extreme value analysis is not necessary, overruling the correlation of water level and wave height.

The urban scale model is forced at the coastline by the total water level  $\eta_{TOT}$ , that is the sum of water level due to storm surge  $\eta$  and wave runup  $R_{2\%}$  (which includes wave setup). More specifically, for each of the analysed sites, the time series of water level obtained by the downscaling procedure with SHYFEM is summed to the wave runup obtained from the following Equation 6 (Atkinson et al., 2017);

$$R_{2\%} = 0.92 \tan \beta \sqrt{H_s L_p} + 0.16 H_s \quad (6)$$

where  $\tan \beta$  is the beach slope,  $H_s$  is the significant wave height and  $L_p$  is the wave length computed by the WaveWatch III model. The extreme value analysis procedure to obtain return period values is then applied to  $\eta_{TOT}$ . To simulate a specific return period event, a triangular synthetic hydrograph with peak equal to the return period value and duration (base of the triangle) assumed equal to 18 hours, is used as the coastal boundary condition for the HEC-RAS model.

### 3 STUDY CASES AND RESULTS

In the following section, we describe the case studies for four frontrunner cities involved in WP3 of the project: Samsun, Massa, Oarsoaldea, and Villanova i la Geltrú. The first case study, conducted by the University of Samsun, tested the full adoption of the two “last-mile” models (HEC-RAS and XBeach) in the pilot area to develop flood maps. The other three case studies, carried out by LaMMA, create datasets supportive for other project components of WP3, WP6, WP7, and WP8, and are part of a common subset of datasets.

However, the downscaling methodologies used for the Samsun case study differ from those used for the other three cases. Therefore, only the Samsun case study includes downscaling methodologies different from the methodologies described in the deliverables for task WP3.2 (D3.3 and D3.4) and adopted in the other three study cases. Nevertheless, SCORE’s objective is to test alternative methods for climate forcing within an identical modelling framework for task 3.4 considering the participation of different partners for each CCLL to demonstrate the general applicability of these models in generating urban-scale flood scenarios.

#### 3.1 Samsun CCLL



Samsun province is located within Türkiye's northern region, the Central Black Sea Region. It is bounded by the Black Sea in the north, Sinop and Çorum in the west, Ordu in the east, and Amasya and Tokat provinces in the south. The province is located at Latitude 41.279 and Longitude 36.352. The coastal areas of Samsun province have a typical Black Sea climate. However, the influences of continental climate prevail in the interior. In general, Samsun receives less precipitation than the Eastern Black Sea and has higher temperatures. The coasts are mild in winter, misty and cold in the spring, and dry in the summer. Precipitation usually takes the form of rain (Demir and Ülke Keskin, 2019). According to the observations of Samsun Regional Meteorological Station (No.17030) in the period 1929-2023, the average annual total precipitation is 723.2 mm, and the maximum annual average temperature is 14.6 °C (MGM, 2024). Samsun province, on the one hand, is one of the most developed and development priority regions of the Black Sea Region in terms of education, health, industry, trade, transportation, and economy, and on the other hand, it is a province where floods occur because of instantaneous rains and snowmelt, especially in the summer months. Past floods threaten the region's people, structures, and underground systems (Demir and Kisi, 2016; Demir and Ülke Keskin, 2020; Beden and Ülke Keskin, 2021; Ülke Keskin et al., 2023). The region's precipitation trends showed a non-statistically significant increase in annual total precipitation (Beden et al., 2020; Korkmaz and Efe, 2021). The main areas of high ecological value in Samsun are the Kızılırmak, Yeşilirmak and Terme deltas, including the Bafra and Çarşamba plains, and the beaches, rocky shores and coastal cliffs of the Terme Coastline (Rebollido and Iglesias, 2023). The land cover of CCLs and Samsun CCLL is shown in Figure 4-5.

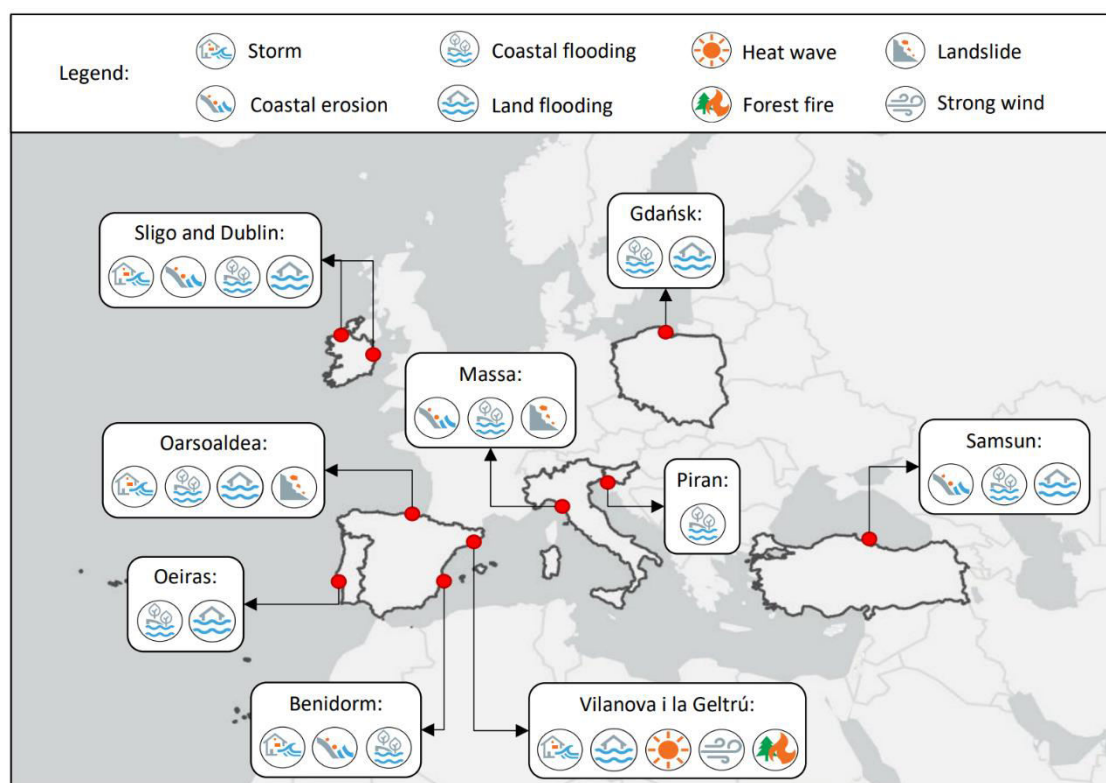




Figure 4. Schematic representation of the main hazards identified for the ten CCLs (Rebollido and Iglesias, 2023).

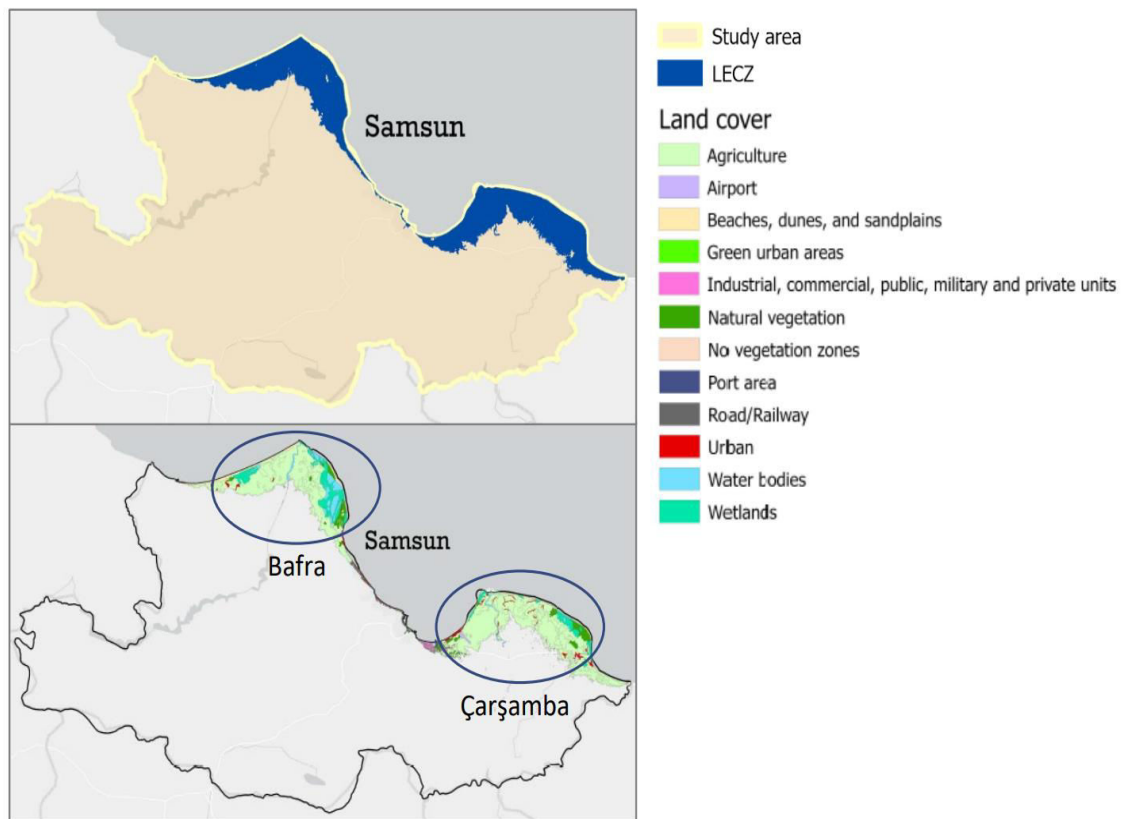


Figure 5. Samsun CCLL and its land cover (Rebollido and Iglesias, 2023).

The study area of the Samsun CCLL is the Kızılırmak Delta. It is also known as Bafra Plain, and it consists of the delta plain and the wetlands formed by the alluviums carried by Kızılırmak where it flows into the Black Sea. The primary problem in the Kızılırmak Delta is coastal erosion and coastal shoreline change (Rebollido and Iglesias, 2022). In addition, coastal and land floods are major disasters in the region. The most important aspect of this area is that it is a Ramsar area, which must be protected. The Kızılırmak delta, produced by the fertile alluviums brought by the Kızılırmak River, is a very important agricultural area and contributes significantly to the economy of the region and country. As a result, agricultural stress, coastal erosion, and fertile soil degradation pose significant risks to the region. Moreover, the expected sea level rise in the Black Sea disrupts both the water quality and ecosystem balance in the lagoons in the Kızılırmak delta, which is the habitat and protection area for many rare species (Rebollido and Rodríguez, 2021). Kızılırmak basin and delta are shown in Figure 6.



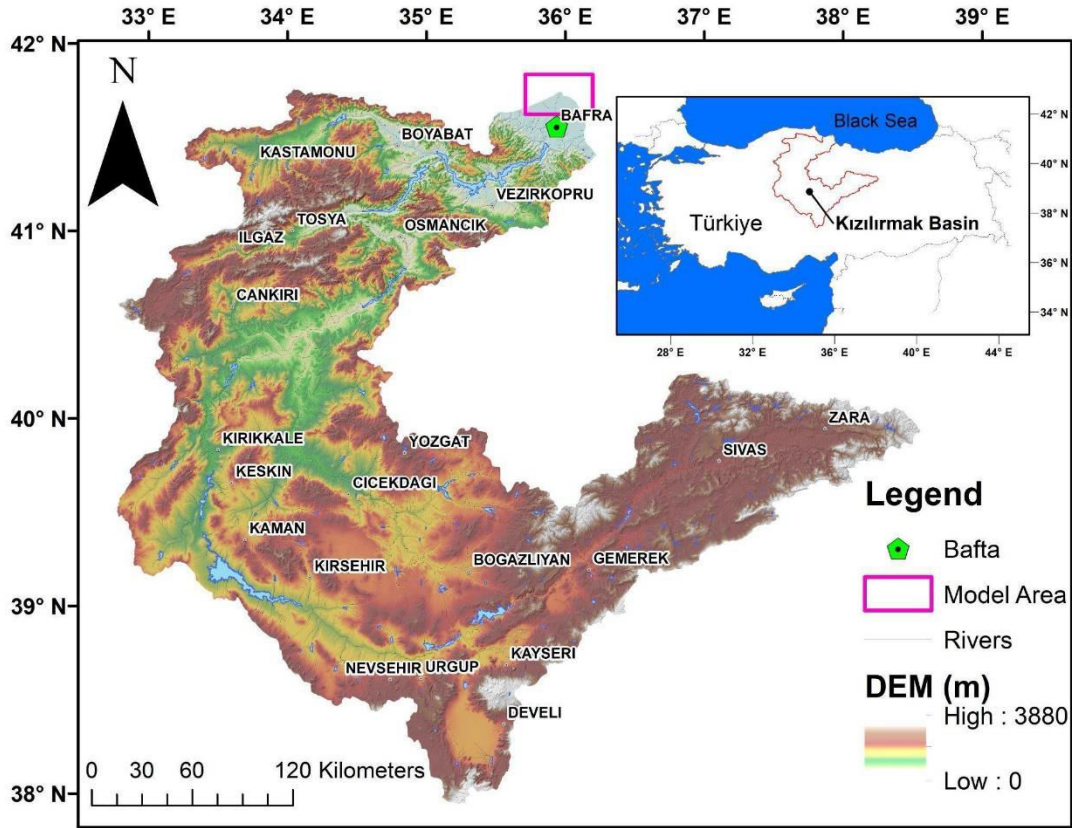


Figure 6. Kızılırmak Basin and Bafra Plain.

As seen in Figure 6, the Kızılırmak river flows through Samsun province to the Black Sea. The Bafra Plain, which is the flood modelling area in this project, is a district of Samsun province. It is a settlement 20 kilometers away from the Black Sea, approximately 20 meters above sea level, and founded on the sediment plain accumulated by the flow in the Kızılırmak Basin. The digital surface model of the study area is shown in Figure 7.

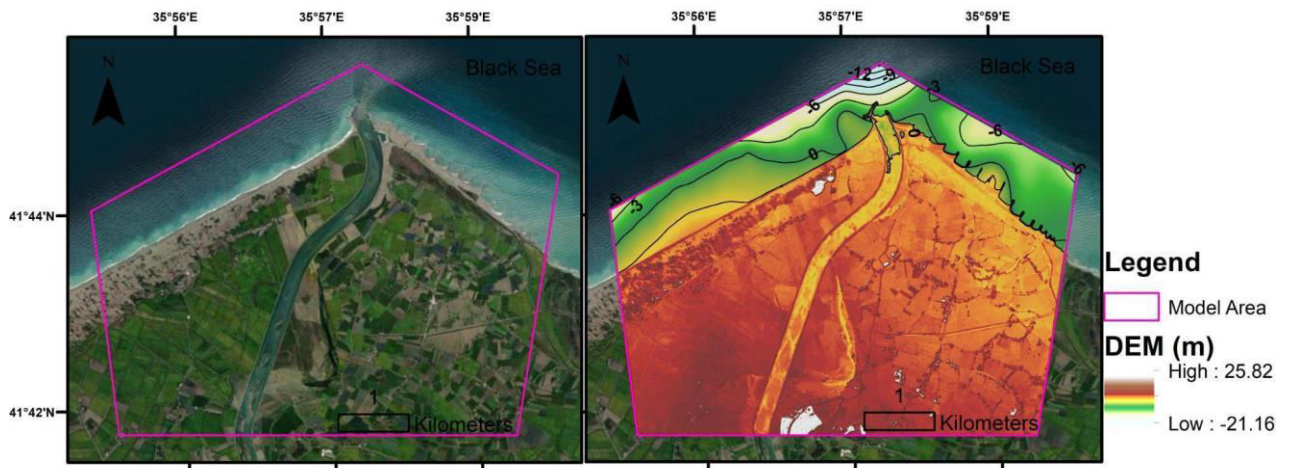


Figure 7. DEM of the flood model area.

### 3.1.1 Meteorological data

Precipitation data of Bafra meteorological station (No.17622) was used in the historical part of the





hydrological modelling of the study. Descriptive statistical information of the data is given in Table 5. The station location is shown in Figure 8.

Table 5. Descriptive statistical information about precipitation and temperature data.

Statistics	Precipitation (mm)	Temperature (°C)
Average	63.566	13.984
Standard Error	1.907	0.269
Median	55.750	13.650
Standart Deviation	45.279	6.386
Kurtosis	4.027	-1.260
Distortion	1.502	0.078
Minimum	0	1.700
Maximum	343.900	25.700

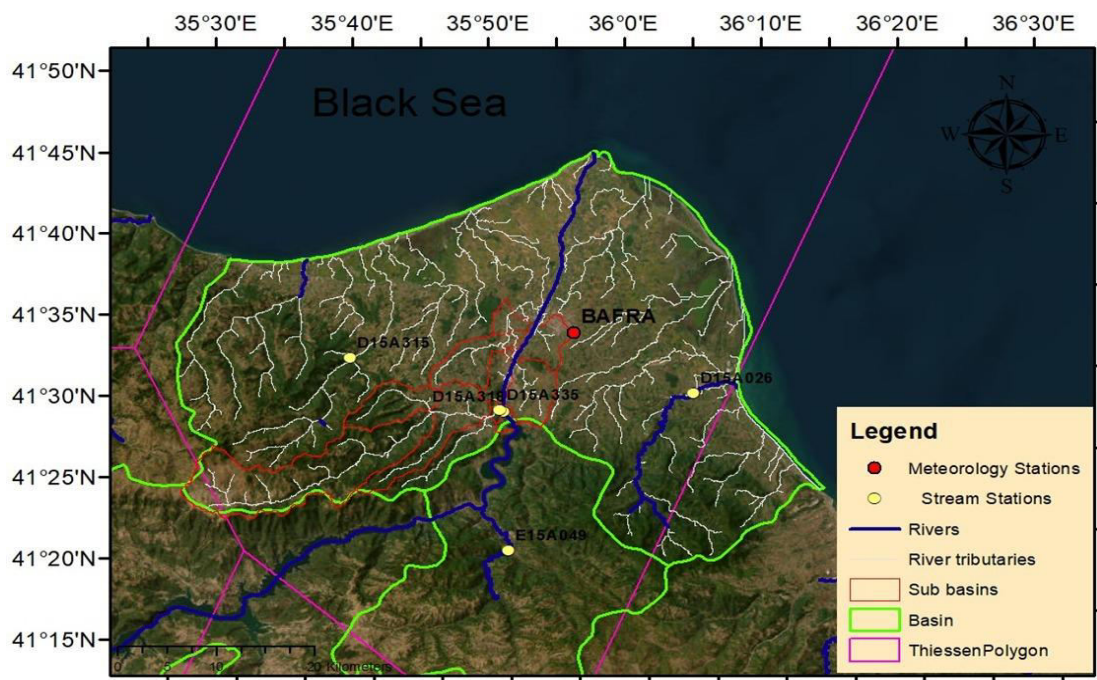


Figure 8. Thiessen polygons and meteorological station location.

Table 5 shows the statistics of the records of Baфра station (17622) between 1976 and 2022, showing that the highest monthly total precipitation data recorded in the region was 343.9 mm and the highest monthly average temperatures was 25.7 °C. High and positive deviations in precipitation indicate that there may be a trend in the data and its homogeneity may deteriorate over the years. Additionally, considering the Thiessen polygons, it can be seen that the examined station is within the boundaries of the study area. Monthly changes in long-term precipitation-temperature data are shown in Figure 9.



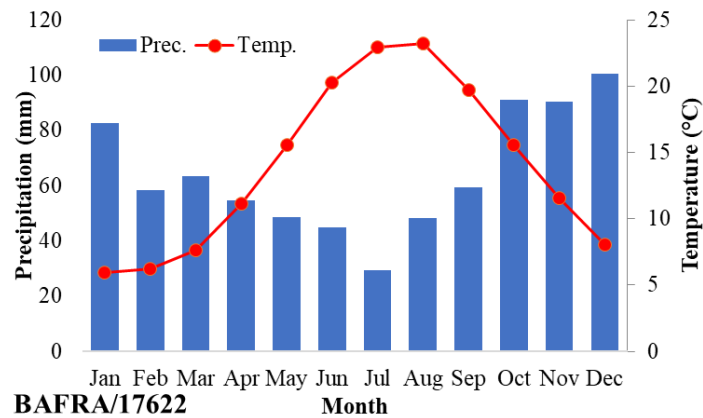


Figure 9. Monthly precipitation and temperatures over 1976 and 2022 as recorded in the Bafra station.

Figure 9 shows that average temperatures reach the highest values in June-July and August and total precipitation reaches the highest values in October-November and December. In addition, when past floods in the region are examined, it is seen that floods generally occur in the summer months as a result of ground moisture saturation due to sudden snowmelt or as a result of sudden rains (Demir and Ülke Keskin, 2020; Beden and Ülke Keskin, 2021).

### 3.1.2 Future Scenarios - RCP 4.5 and RCP 8.5

Representative concentration pathways (RCP) portray possible future greenhouse gas and aerosol emissions scenarios. RCP scenarios are defined by the total solar radiative forcing by 2100. RCP 4.5 is described by the Intergovernmental Panel on Climate Change (IPCC) as a moderate scenario in which emissions peak around 2040 and then decline. It represents a stabilization scenario where policies and measures are implemented to reduce emissions, leading to a moderate radiative forcing ( $4.5 \text{ W/m}^2$ ) by 2100. RCP 8.5 assumes that emissions will continue to rise throughout the 21st century without significant mitigation efforts, leading to a high level of radiative forcing ( $8.5 \text{ W/m}^2$ ) by the year 2100. Therefore, climate change projected under RCP 8.5 will typically be more severe than under RCP 4.5. These scenarios help scientists and policymakers understand the potential impacts of different levels of greenhouse gas emissions on global temperatures, sea levels, and other climate-related factors over the long term. By comparing these scenarios, researchers can assess the effectiveness of mitigation strategies and the urgency of implementing them to limit climate change impacts.

### 3.1.3 CORDEX

Regional climate downscaling (RCD) techniques, including dynamical and statistical approaches, are increasingly used to provide higher-resolution climate information than is available directly from contemporary global climate models. The techniques available, their applications, and the community using them are broad and varied, and it is a growing area. However, it is important that these techniques, and the results they produce, are applied appropriately and that their strengths and weaknesses are



understood. This requires a better evaluation and quantification of the performance of the different techniques for application to specific problems. Building on experience gained in the global modelling community, a coordinated, international effort to assess and intercompare various RCD techniques objectively will provide a means to evaluate their performance, illustrate the benefits and shortcomings of different approaches, and provide a more solid scientific basis for impact assessments and other uses of downscaled climate information.

The World Climate Research Programme (WCRP) views regional downscaling as both an important research topic and an opportunity to engage a broader community of climate scientists in its activities. The Coordinated Regional Climate Downscaling Experiment (CORDEX) has catalyzed the achievement of this goal.

Daily total precipitation data from the CORDEX simulates future precipitation simulations. For the current study, the selected MNA-44 domain, covers all parts of Turkiye. CNRM-CERFACS-CNRM-CM5 is used as the driving model. The RCP8.5 and RCP4.5 experiment is used to obtain future simulations for the period 2006 - 2100. And the RCA4 model is used for dynamical downscaling. The obtained RCP4.5 and RCP8.5 data were transferred to the Easyfit program (<https://easyfit.en.softonic.com/>), and future precipitation scenarios were made for various return periods. The further details are given in Table 6.

Table 6. Details of the CORDEX precipitation data for Turkiye.

Variable	Precipitation
Time-Frequency	Daily
Domain	MNA-44
Model Latitudinal Boundaries	-6.60 – 44.88
Model Longitudinal Boundaries	-26.40 – 75.24
Driving Model	CNRM-CM5 (Centre National de Recherches Meteorologiques-Climate Model)
Experiment	RCP8.5, RCP4.5
Regional Climate Model (RCM)	Rosby Centre Regional Atmospheric Model (RCA4)

### 3.1.4 Hydrological modelling

Hydrological modelling aims to find the required flow hydrograph for the hydraulic model. For this purpose, various statistical distributions and their suitability tests based on the rainfall-runoff relationship are performed. The maximum precipitation value in the relevant year is obtained by considering the maximum of the daily average precipitation values obtained during the year. At least 30 years of observed data sets are needed to reach meaningful statistical results in hydrological modelling. Observational data



can be obtained from various meteorological services. Several sources for downloading and viewing data allow you to subset the data to only include specific parameters and/or geographic locations. For hydrological modelling, daily total maximum precipitation data is required. After this value is obtained throughout the studied period, it complies with statistical distributions, modelling with historical data, modelling with a moderate radiative forcing scenario (RCP 4.5), and modelling with a warming scenario (RCP 8.5). The flow chart of hydrological modelling is shown in Figure 10.

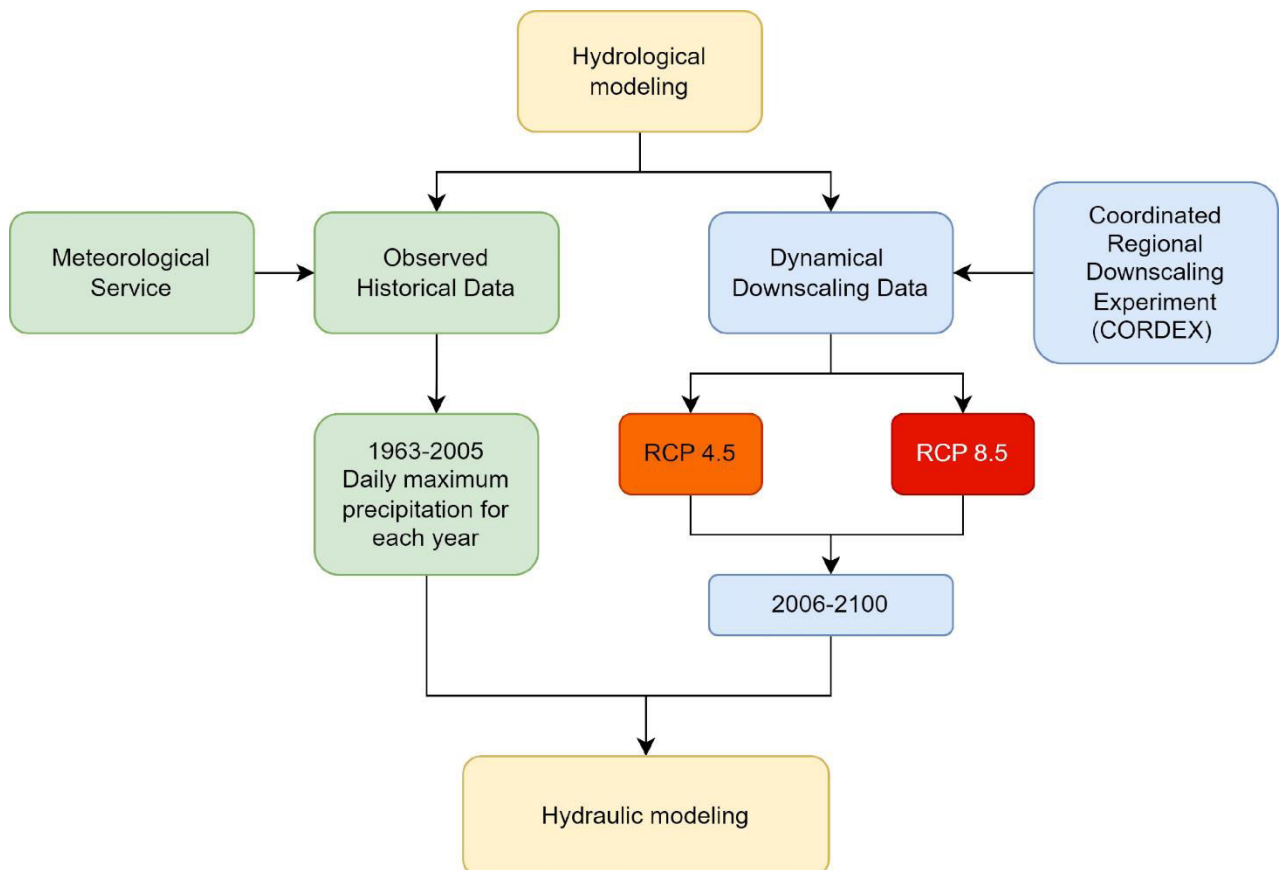


Figure 10. Flow chart of hydrological modelling.

The Normal distribution, Log-Normal (2 Parameters), Log-Normal (3 Parameters), Pearson Type-3 (Gamma Type-3), Log-Pearson Type-3, and Gumbel distributions were used to find the best suitable statistical distributions. The suitability test of distribution types was carried out with the Kolmogorov-Smirnov test. The hydrological modelling as presented in Figure 10 was carried out in two stages. In addition, for 1D land flood modelling, the adequacy of river cross-sections with Log-Normal (3 Parameters) distribution for annual maximum instantaneous flows between 2009 and 2020 was investigated. Table 7 shows the return periods of 1D modelling.

Table 7. Return periods of 1D modelling.



Return Period	2	5	10	25	50	100	200	500	1000	10000
Log Normal (3P)	268.3	326.57	370.33	431	479.87	531.75	586.93	665.37	729.14	971.23
Weibull (3P)	267.95	301.44	316.92	332.11	341.29	349.17	356.08	364.11	369.53	384.7
Gumbel	273.16	338.32	381.46	435.97	476.4	516.54	556.53	609.3	649.17	781.57
Log Normal	278.26	333.05	365.85	404.4	431.43	457.29	482.32	514.48	538.32	615.67
Log Pearson	264.62	325.92	375.39	448.02	509.79	578.51	655.12	770.31	869.46	1291.4
Normal	285.27	347.33	379.76	414.35	436.7	456.8	475.19	497.48	513.12	559.48

In Table 7, when the flow rates were modelled as 1D, it was seen that the cross-sections were insufficient for the Q25 flow rate (Figure 11). For this reason, hydrological modelling was carried out through 2D modelling.

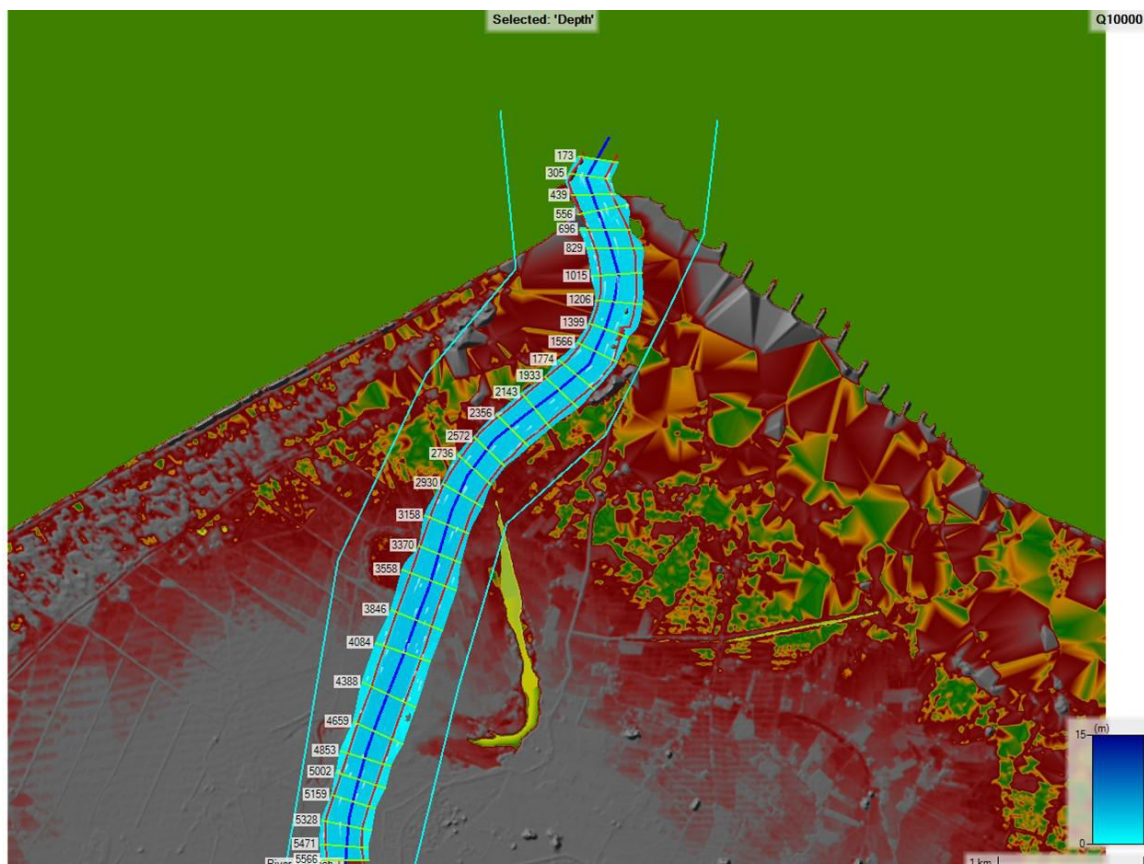


Figure 11. River cross sections and 1D modelling.

In 2D hydraulic modelling, the first thing to do is to determine data distributions by using historical data





from meteorological stations (daily maximum precipitation between 1963-2005) and to determine the recurrent flows of these distributions (Figure 12). The second stage was carried out using Dynamic Downscaling data based on CORDEX data, using. Two different scenarios (RCP 4.5 and RCP 8.5) and repeated flows were obtained in various sub-periods between 2006 and 2100, as a continuation of historical data (Table 8). These data are input data for hydraulic modelling.

Table 8. Summary of hydrological modelling results.

Data Modelling	Year/Return	10000	1000	500	200	100	50	25	10	5	2
Historical	1963-2005	837.93	683.03	638.03	583.66	535.39	492.27	449.90	394.96	354.10	298.63
RCP 4.5	2006-2100	441.09	398.74	382.32	361.47	350.50	334.71	318.60	296.66	279.18	253.99
	2015-2065	467.90	415.85	395.55	371.44	356.68	337.68	318.77	293.74	274.64	249.12
	2045-2095	451.60	402.34	385.07	367.15	354.36	339.47	324.19	303.01	285.80	259.95
RCP 8.5	2006-2100	690.90	551.91	506.15	474.41	429.41	395.47	363.80	324.59	296.60	260.57
	2015-2065	573.40	477.57	449.91	420.32	389.90	365.20	341.16	310.18	286.86	255.33
	2045-2095	677.26	551.88	509.80	477.40	438.23	405.76	374.88	335.74	307.02	268.55



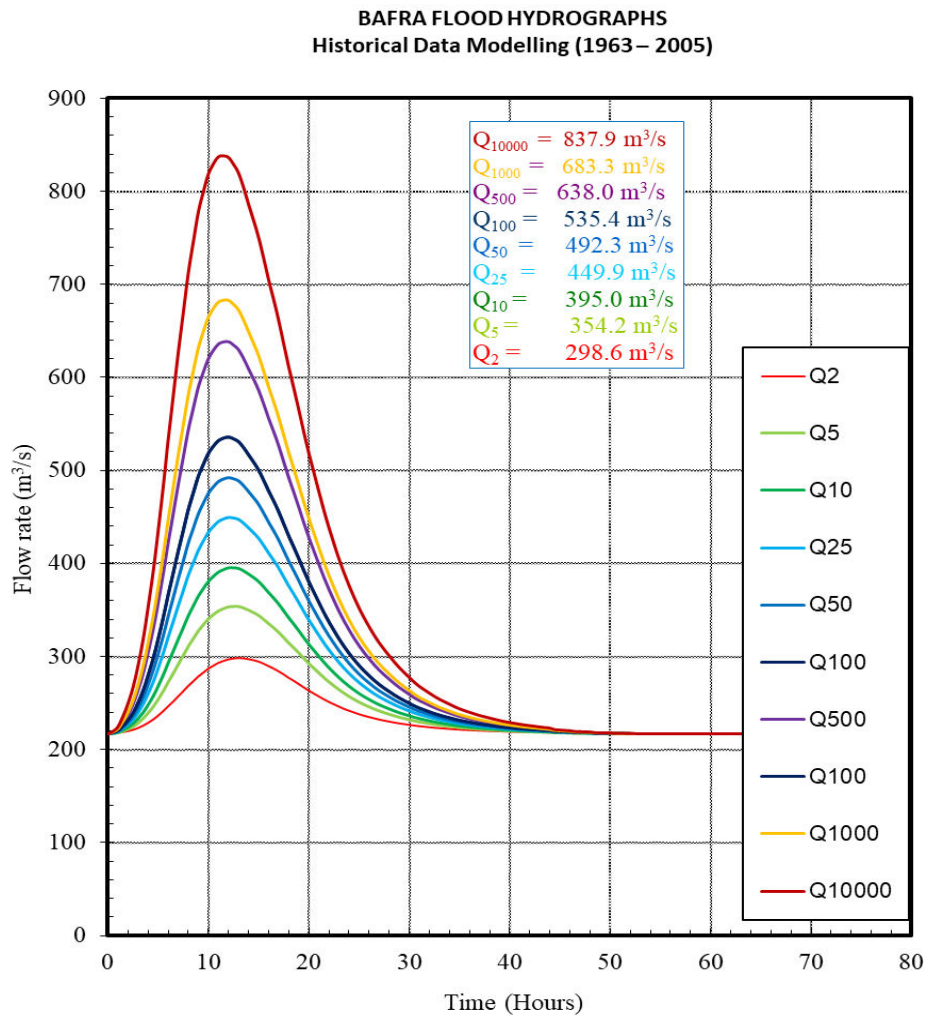


Figure 12. Flood hydrographs for different return periods.

### 3.1.5 Hydraulic modelling results

#### 3.1.5.1 Land flooding results

The HEC-RAS can simulate both 1D steady flow and 2D unsteady flow. HEC-RAS analysis flow over a river network using geometric and hydraulic calculation processes (Lea et. al, 2019; Demir et. al, 2021). In this section, the Bafra Basin, near Samsun, and the land flood propagation and velocity mappings were examined using HEC-RAS (2D unsteady flow). Model results were obtained according to the EU flood directive "floods with a medium probability (likely return period  $\geq 100$  years)" as well as maps for standard Q25, Q50, Q100 and Q500 flood recurrence periods (Floods Directive, 2018). Flood maps showed that much of the region was highly affected by flood events/s during the 25-year return period (Q25).



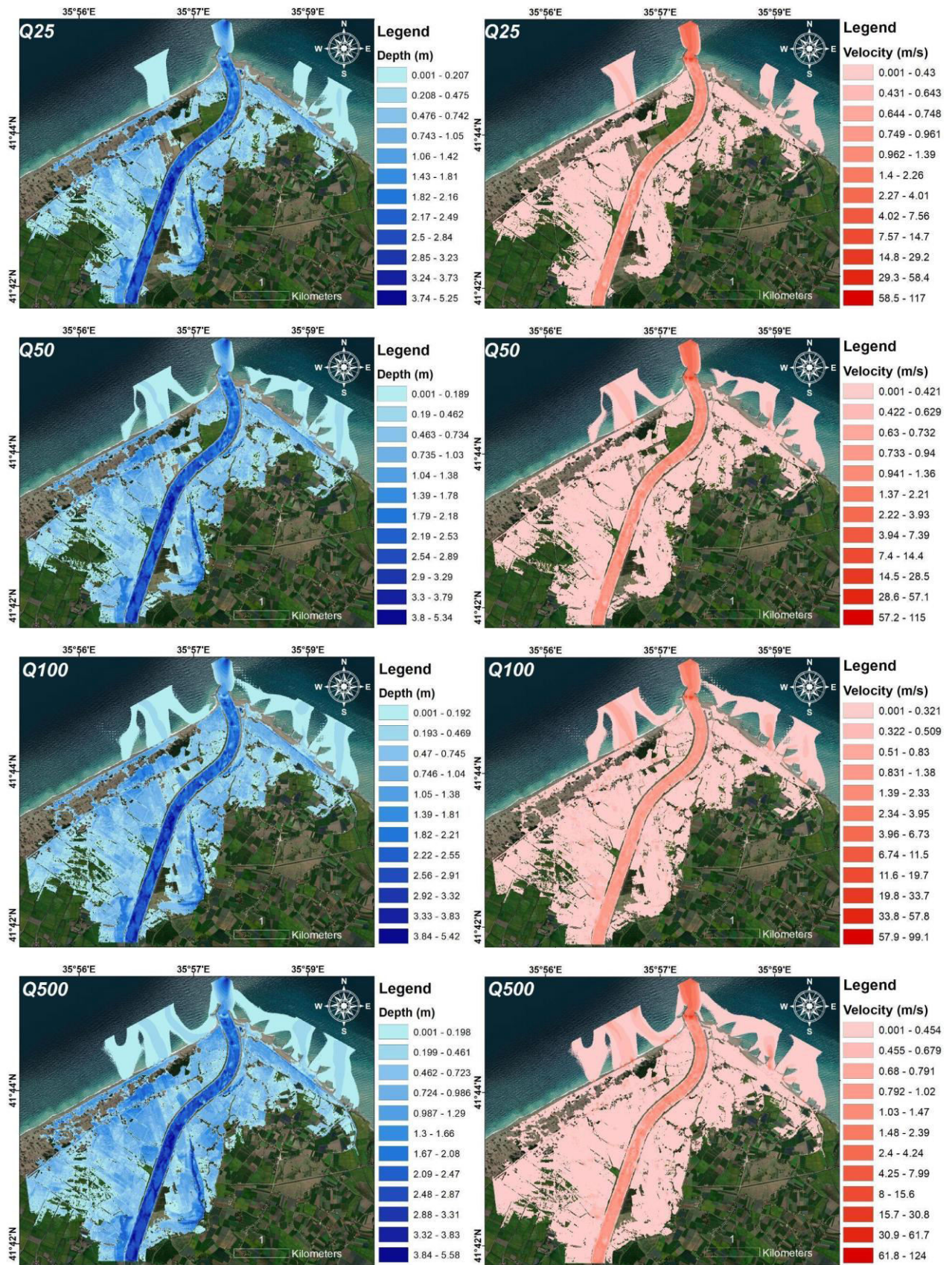


Figure 13. Flood propagation and water velocity maps for different periods (historical land flood modelling).



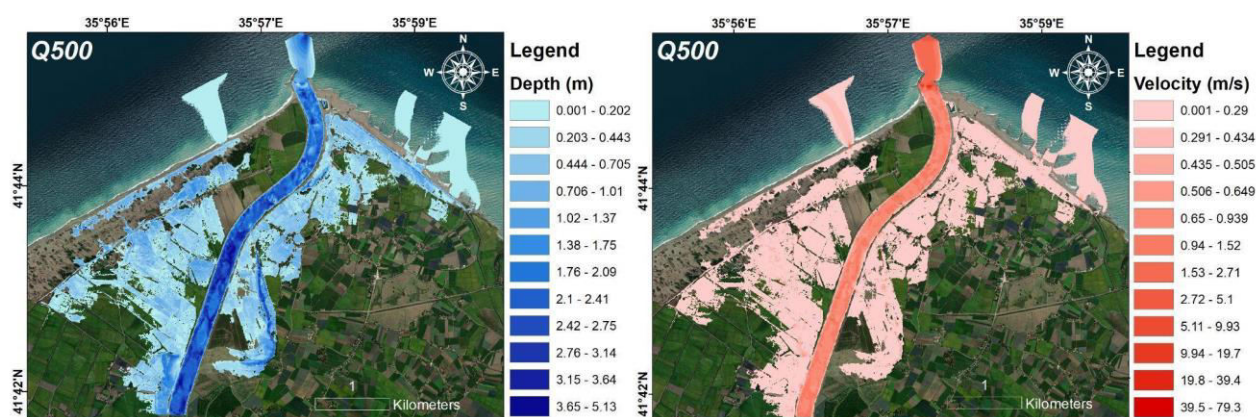


Figure 14. Flood propagation and water velocity maps for different periods (RCP 4.5).

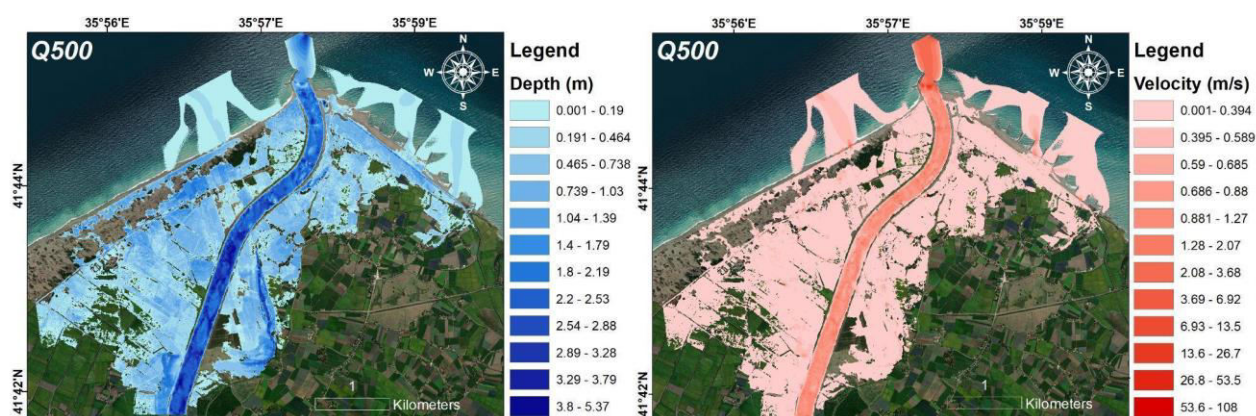


Figure 15. Flood propagation and water velocity maps for different periods (RCP 8.5).

The maps in Figures 13, 14 and 15 were obtained using the recurrence discharges listed in Table 8. In the models, the highest velocities and water levels are observed in the middle regions of the river. This indicates that the water, which cannot be contained within the river cross-section, overflows and spreads to the surrounding areas. Specifically, the areas where the most water spreads are observed in the models using historical data (Figure 13). This is due to the high-value recurrences obtained in the frequency analysis of the historical data. In future scenarios, lower recurrence discharges have been obtained due to the anticipated decrease in regional precipitation in the coming years. However, water spread is still observed in the RCP 4.5 scenario, as shown in Figure 14. When examining the water velocities in the study area, it is seen that the velocities are constant and very low (<1m/s). In areas outside the middle sections of the river, the water moves quite slowly. However, due to an obstacle located at the downstream end of the study area, the water first rises and gains energy in this region. Then, it quickly jumps and flows into the Black Sea. Therefore, water velocities only rise to high levels (>10m/s) in this region. The change in flood spread areas and average velocities according to recurrence discharges obtained from the models is presented in Table 9.

Table 9. Summary of flooded areas and average speeds.

Hydrological modelling	Return Periods	Area (km <sup>2</sup> )	Average Velocity (m/s)
Historical	Q25	8.958	0.130



	Q50	10.30	0.131
	Q100	11.27	0.137
	Q500	12.70	0.143
<b>RCP4.5</b>	Q500	7.49	0.130
<b>RCP8.5</b>	Q500	10.71	0.135

The results of the modelling scenarios Table 9 showed that the average water levels in the study area increased from 0.1 m to 6 m on average and the levels spread over an area from 8.95 km<sup>2</sup> to 12.70 km<sup>2</sup>. In addition, considering that the average velocity in the region was up to 0.140 m/s in order to reduce property loss and prevent potential damage due to flooding, models can be used to manage flood control and simulate flooding in real time. It is envisaged that flood effects in this region can be prevented by cleaning the river bottom and widening river sections. In addition, this floodplain should continue to be used as agricultural land. The Samsun CCLL land flood discussed in this work package was carried out by considering the most extreme events. The base flow value was considered as 217.2 m<sup>3</sup>/s, taking into account the most unfavourable situation seen 95% of the time. From this base flow value, flow rates go up to 638.03 m<sup>3</sup>/s for Q500 flow rate in Historical modelling (1963-2005); and up to 395.55 m<sup>3</sup>/s for Q500 flow rate in RCP 4.5 modelling, while up to 395.55 m<sup>3</sup>/s for Q 500 flow rate in RCP 8.5 modelling. It increases up to 509.80 m<sup>3</sup>/s although flood extents reach up to 12.70 km<sup>2</sup> in the study area, the fact that water velocities are quite low shows that the danger and risk of floods in the region may be low but their spread, coverage of surface area, may be high.

### 3.1.5.2 Coastal flooding results

Following the land flood modelling, coastal flood modelling was conducted using XBeach for a case where a severe storm was observed according to local records (e.g., 14th August 2011). The model was initialized two days prior to the event and operated for a duration of three days. One of the inputs for XBeach, the bathymetry data, was created for the study area by combining the DEM data provided in Figure 7 which has 5m resolution and the GEBCO gridded bathymetry data with 500m resolution. For bathymetry, high-resolution DEM data was utilized up to 1 km offshore, while low-resolution GEBCO data was used for the area extending from this point to the model boundaries. Additionally, model grids were generated with the help of Delft3D, and the bathymetry data for the model area was adjusted (Figure 16). Wave data for boundary conditions were taken from the ERA5 reanalysis dataset, which includes variables such as wave height, wave period, and wave direction. Since tides are not observed in Samsun region, they were not included in the modelling.



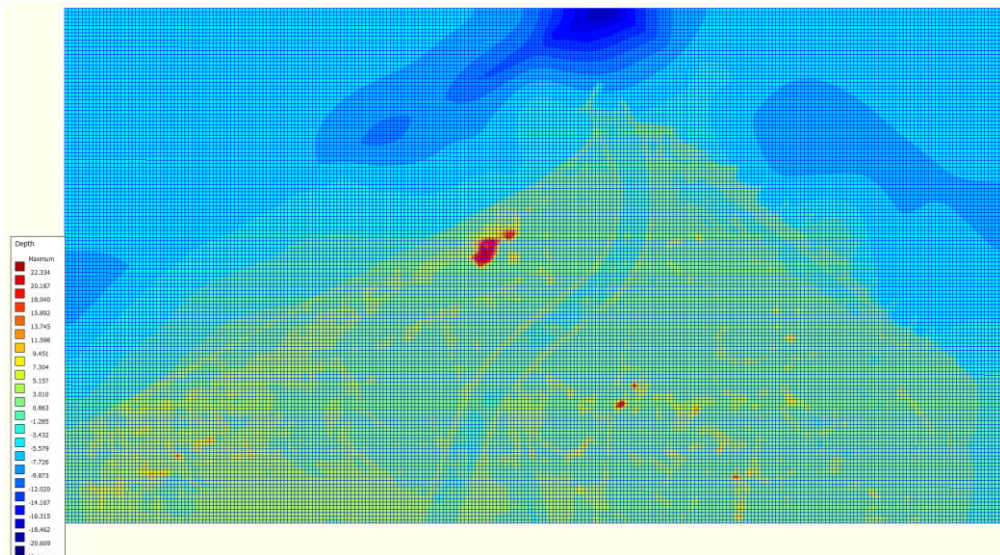


Figure 16. Bathymetry input and grid structure for Xbeach model.

As a result of the modelling with XBeach, the two most prominent variables were water level and wave height. These two variables are shown at various time steps in Figure 17.



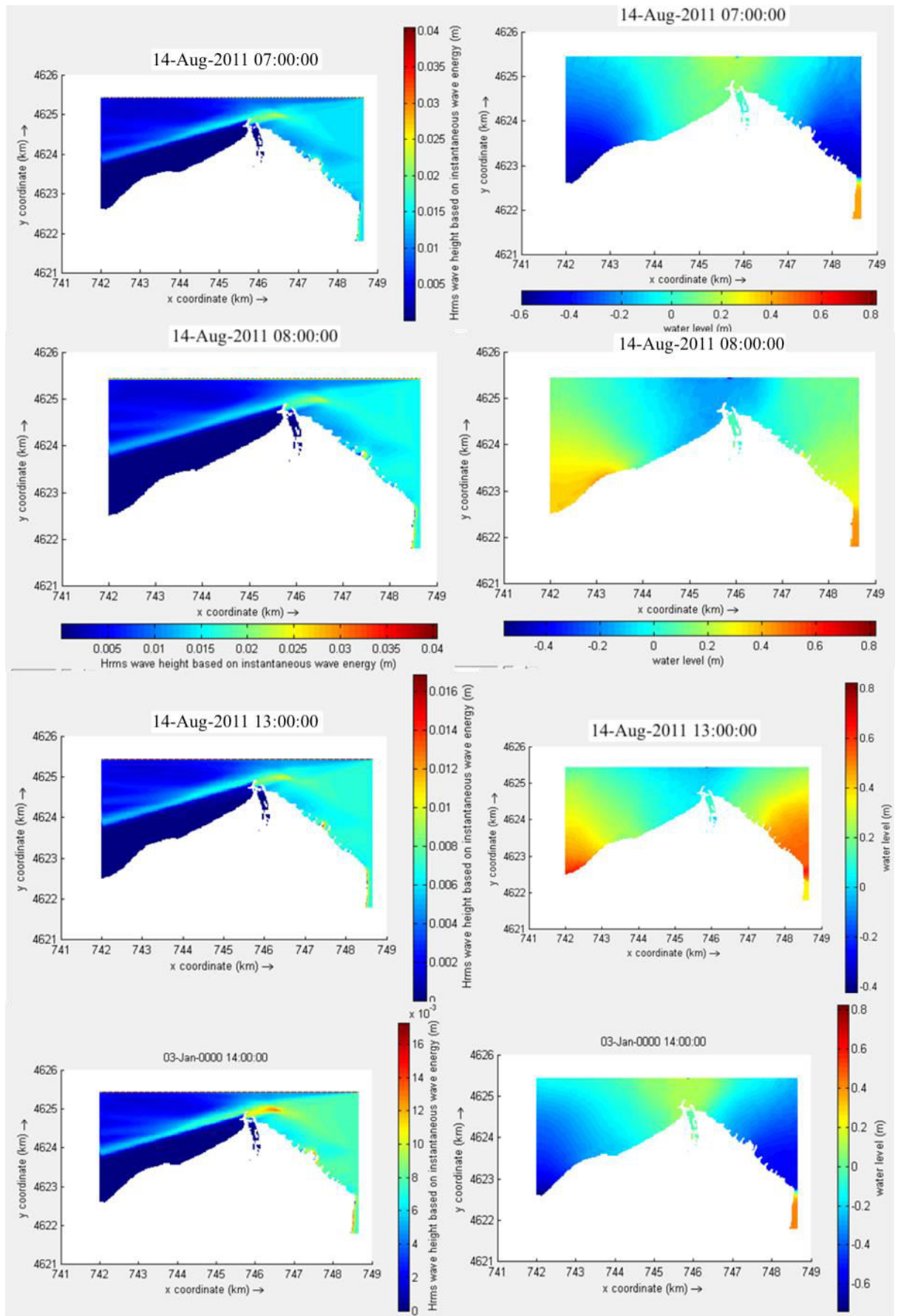


Figure 17. Coastal flood modelling water level and wave height results.





According to the model results at 7 GMT on 14 August 2011, wave height and water level are observed to be greater at the river mouth compared to other regions of the study area. As time progresses, both wave heights and water levels increase. At 8 GMT, while the water level at the river mouth decreases, the water levels along the left and right banks of the river rise. This increase in water level continues until 13 GMT, at which point the maximum water level is observed. Concurrently, as water levels on the left and right banks rise, wave height at the river mouth also increases. Despite these variations in water level and wave height, coastal erosion was not observed in the study area, not even on a day of an extreme event like 14<sup>th</sup> August 2011. As the next step, it is recommended to run the area in 1D and at a higher resolution to assess the potential occurrence of coastal flooding.

### 3.1.5.3 Coupled modelling

The water level results at the coastal boundary from the 2D modelling conducted with Xbeach were used as boundary conditions for the land flood modelling with the HEC-RAS model. This was achieved by extracting cross-sections perpendicular to the coast at intervals from the 2D Xbeach model to obtain water level values at the coastal boundary. The results of the coupled model are shown in Figure 18.

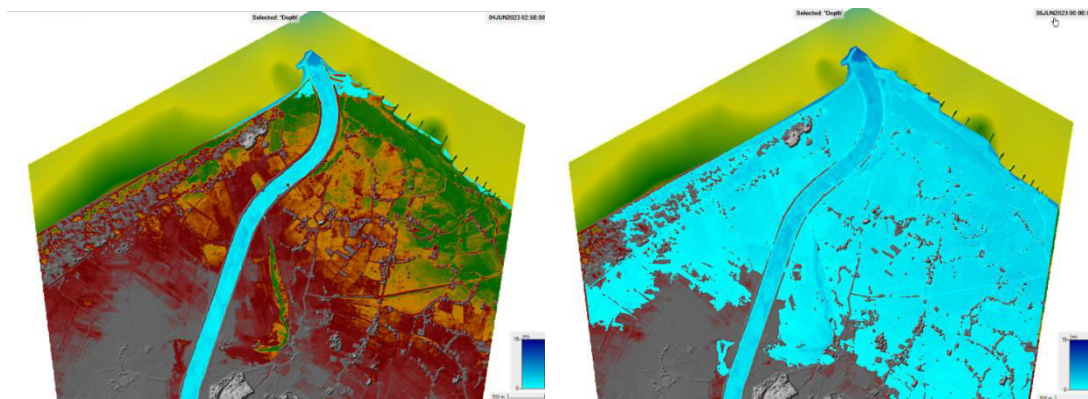


Figure 18. Coupled land and coastal flood modelling results.

## 3.2 Massa

Massa is a coastal city situated in the northern part of Tuscany, along the Tyrrhenian Sea. The city centre of Massa sits at an elevation of 65 meters above sea level. The entire area is intersected by multiple rivers, among which the Frigido River is the main one. The city, which has 70.000 inhabitants and 9 km of coastline, is an appreciated tourist destination because of its characteristic geographical position between sea and mountains. In a few kilometres there is a great variety of landscapes: from the sandy beaches that have been popular since the last century, to the peaks of the Apuan Alps, where the world-famous marble quarries are developed on the western side of the mountain territory, bordering the nearby municipality of Carrara. In Massa's local economy, tourism has played a significant role since the early 19th century. Among the others, the defining feature of the city is its nearly 9 km coastline, with over a dozen artificial cliffs perpendicular to the shore, created to protect the shores from erosion. Stretching from the beach and extending 100 meters into the sea, these cliffs measure between 6 to 10 meters wide and are spaced roughly 200 meters apart.



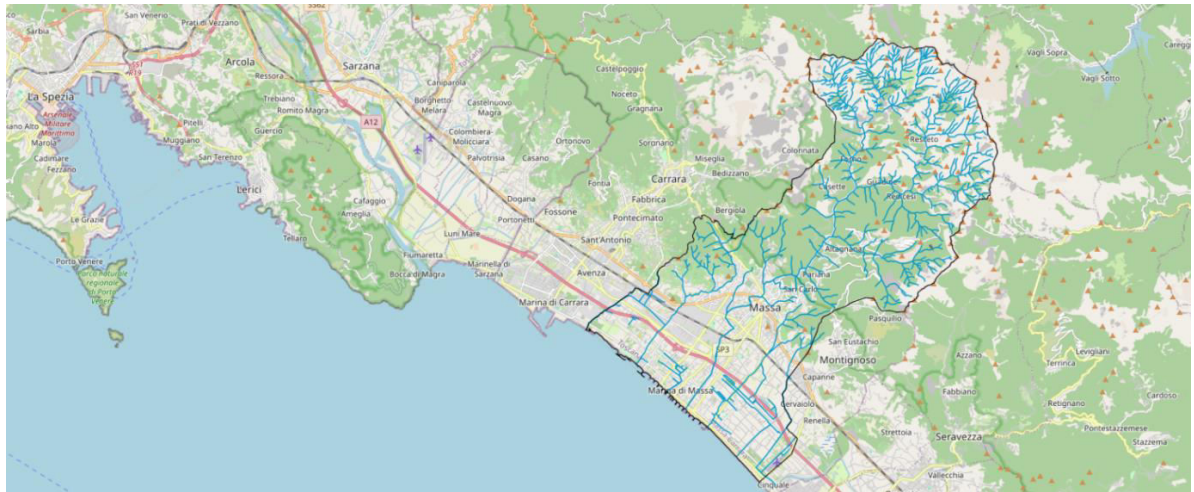


Figure 19. Massa CCLL

The study area of the urban scale flood model consists in the lower part of the municipality, as shown below. A 1D/2D approach was implemented on HEC-RAS where the Frigido river has a 1D geometry with 134 cross-sections defined along the river, each of them with their own bank stations, levees, Manning’s coefficient data. Three different bridges were also defined with the 1D approach.

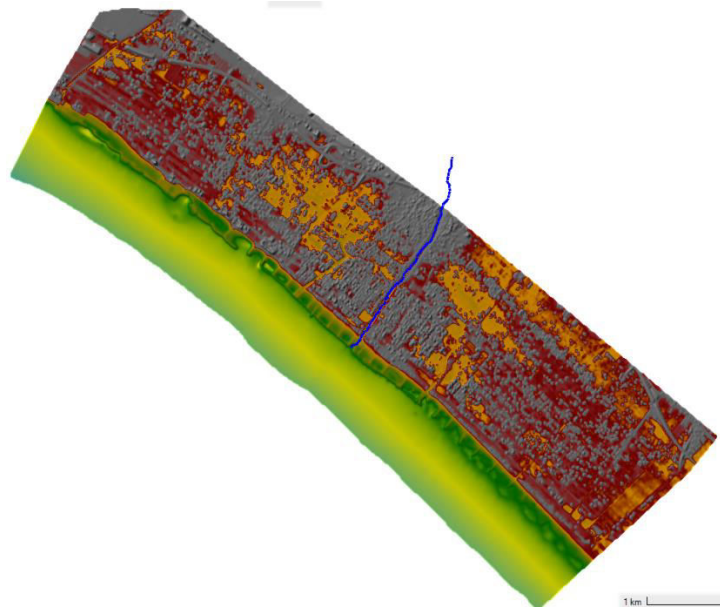


Figure 20. Study area in HEC-RAS with DEM and 1D Frigido river

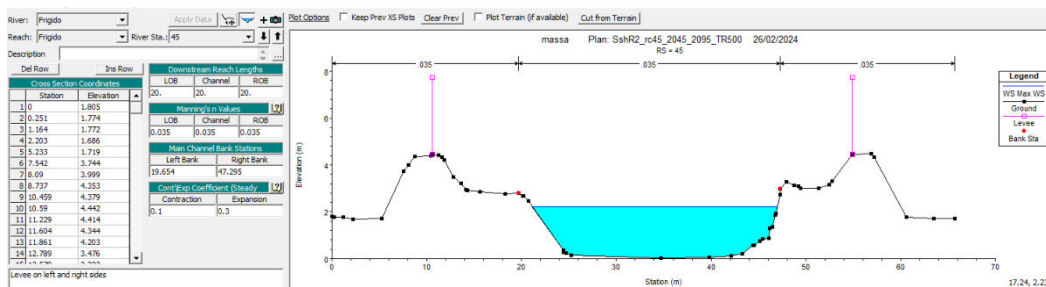




Figure 21. Example of a river cross section in 1D modeling

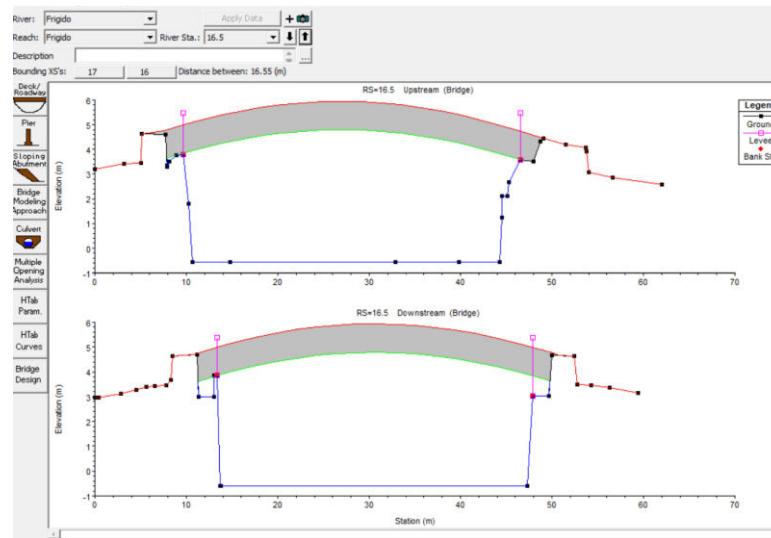


Figure 22. Example of a bridge modeling

To implement the 2D model, a Digital Elevation Model (DEM) of the urban area is needed. Once the DEM is included and connected with the geometry, the 2D Flow Areas, “north” and “south”, were defined in the urban area respectively on the right and on the left side of Frigido, with a spatial resolution of 20x20 meters. Moreover, a 2D Flow Area was added at the mouth of Frigido to create the downstream boundary condition of the river. Finally, the lateral structures were drawn along the riverbanks. They consist in a layer used to locate the centerline of hydraulic structures run parallel to the river course and are used to connect a river reach to a 2D Flow Area, so they represent the connection between the 1D and the 2D approach.

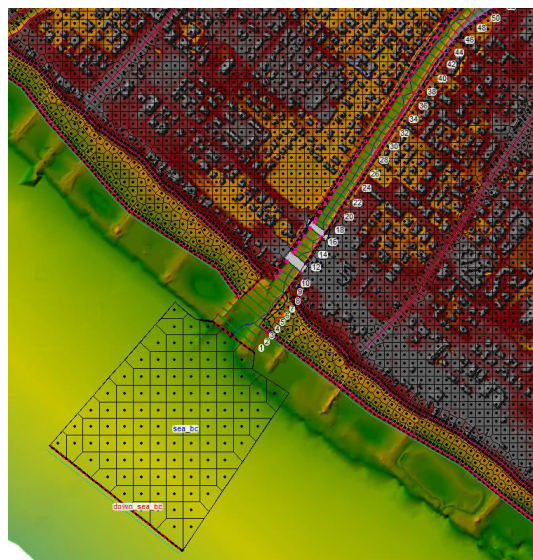


Figure 23. 2D flow area mesh, lateral structures, cross sections

Once the geometry has been completed, input data must be defined editing the “unsteady flow data” section, where the boundary and the initial conditions on both river and 2D Flow Areas are entered based





on the previous model runs (LISFLOOD, SHYFEM, WWIII) and the extreme value analysis results. In this case, the initial condition on the river's most upstream cross section is a flow of  $15 \text{ m}^3/\text{s}$ , while the initial elevation of the 2D Flow Areas is  $-1 \text{ m}$ . That is because the DEM has some points where the terrain elevation is lower than  $0 \text{ m}$ , and it is necessary to prevent flooding just for a matter of initial conditions.

Two types of simulations were carried out: river and coastal floods. The first one involves simulating a flood event from the river, with a hydrograph, while the sea level remains constant. The hydrograph is the result of the extreme value analysis and the hydrological model. The second case simulates a major sea event by fluctuating the water level, while the river maintains a constant flow. The sea water level variation depends on storm surge, tide, wave runup and increase of relative mean sea level (only for future scenarios).

Finally, the unsteady flow simulations for river and coastal flood were carried out, which consist in 5 different scenarios: the historical (1956-2005) that represents the current climate situation, and the future scenarios, RCP 4.5 near future (2015-2065), RCP 4.5 remote future (2045-2095), RCP 8.5 near future (2015-2065) and RCP 8.5 remote future (2045-2095). Each scenario includes 5, 25, 50, 100, 200 and 500 years return periods, for a total of 60 simulations.

## RESULTS – RIVER FLOOD

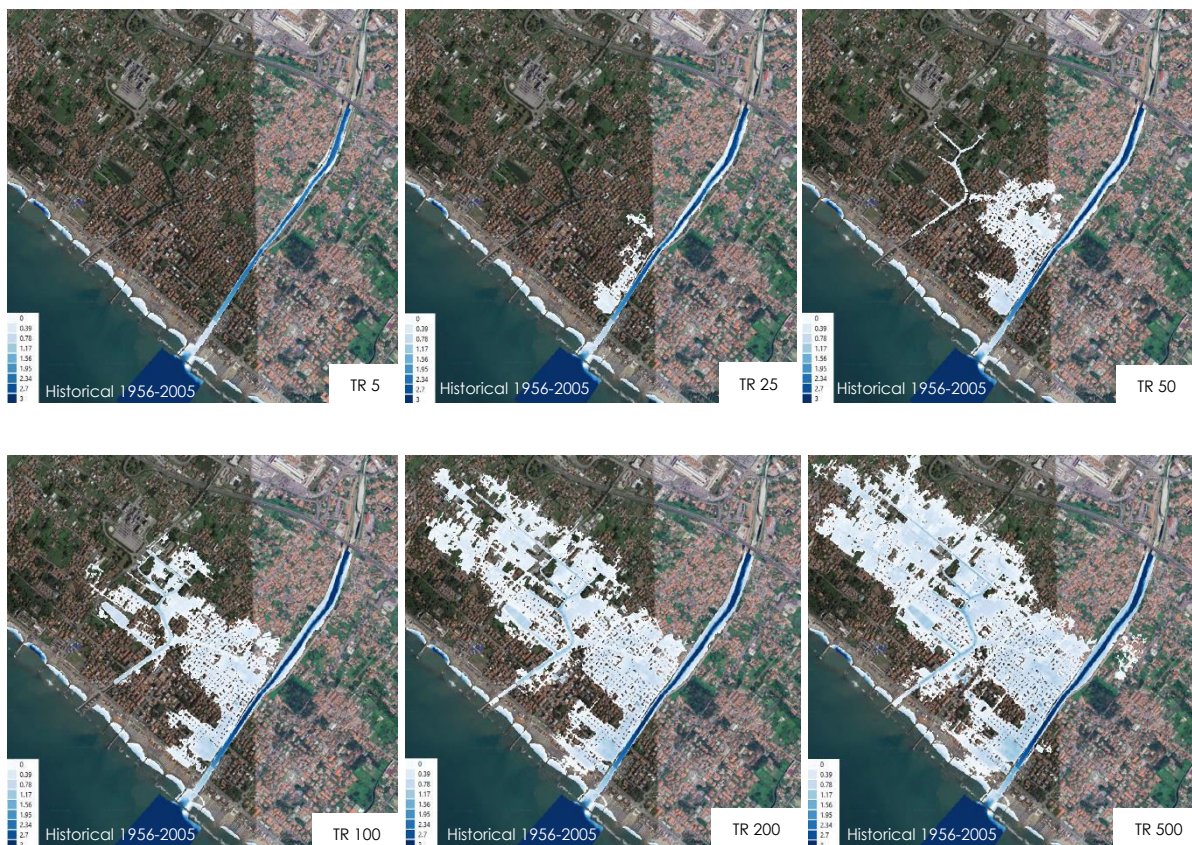


Figure 24. Hazard maps for river flood, return periods 5, 25, 50, 100, 200, 500 years, Historical 1956-2005



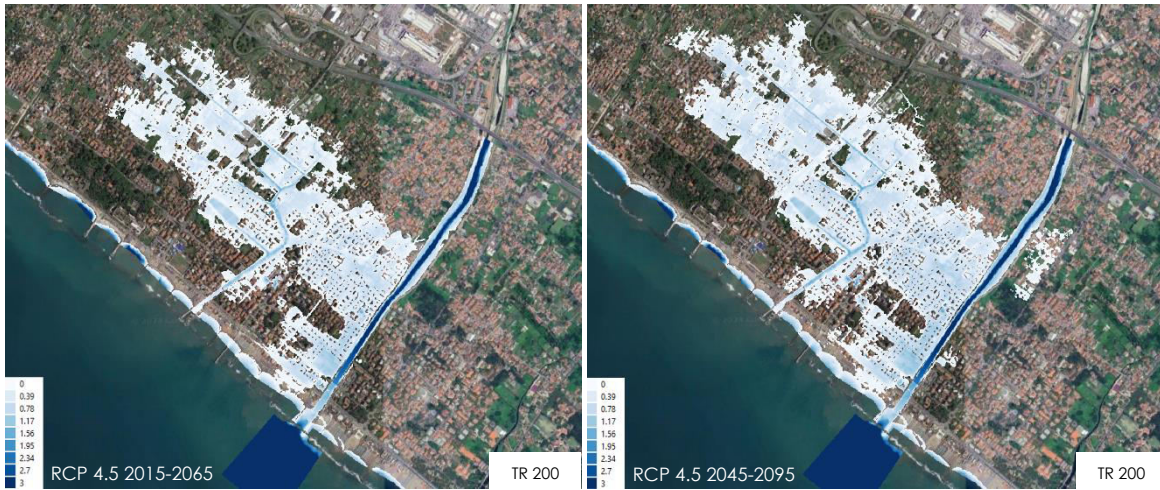


Figure 25. Hazard maps for river flood, return period 200 years, RCP 4.5

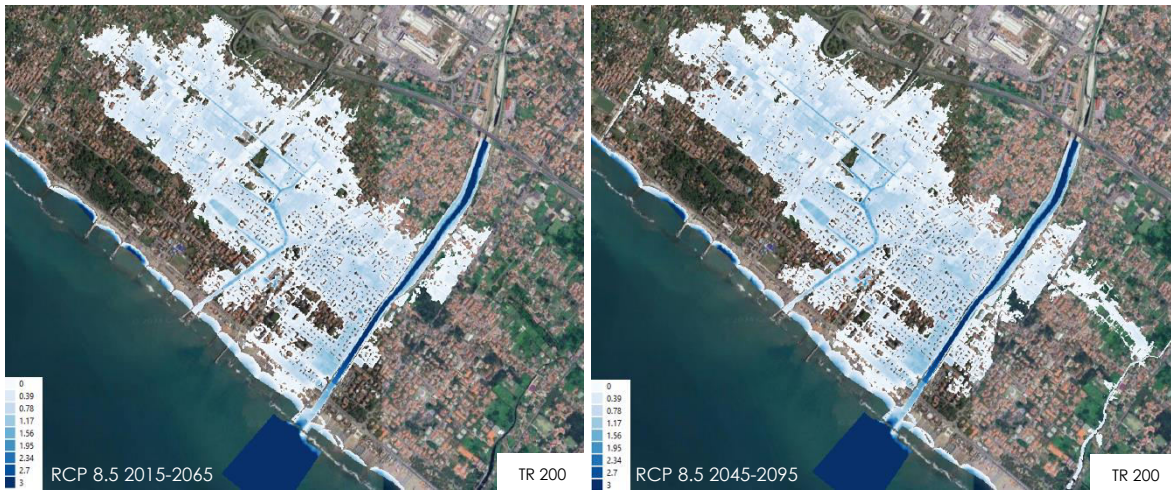


Figure 26. Hazard maps for river flood, return period 200 years, RCP 8.5

**RESULTS – COASTAL FLOOD**





Figure 27. Hazard maps for coastal flood, return period 500 years, Historical, RCP 4.5, RCP 8.5

It is important to note that future scenarios will lead to a worsening of the flood situation, both for river and coastal floods, compared to the historical scenario. Moreover, the RCP 8.5 scenarios result in a more extended flooded area compared to the RCP 4.5 scenarios.

As for coastal events, they can cause flooding in the urban area due to the presence of canals that overflow because of high water level. The historical scenario shows that, even for event with a very high return period (500 years), coastal flood is very limited. On the other hand, in the future the flooded area caused by extreme coastal events will be comparable to that of a river flood. This result is very significant and, as we will see, it is not common with the other cities.

## EBAs

Ecosystem-based approaches (EBAs) are green solutions to help restore ecosystems. During the EBA workshop in Massa, the CCLL team met the community members to identify the main environmental hazards for the region (given the previous SCORE achievements) and priorities the most relevant Ecosystem-based approaches for the Massa community. EBAs are kind of solutions that help protect communities against environmental hazards and, furthermore, can provide co-benefits, including job opportunities, improved water quality and biodiversity. Through the former co-creation workshop, community members concluded the following EBAs were most relevant to the Massa CLL:

- Riparian reforestation: A riparian forest or riparian woodland is a forested or wooded area of land adjacent to a body of water such as a river, stream, pond, lake, marshland, estuary, canal, sink or reservoir.
- Floodplain enlargement: A floodplain or flood plain is an area of land adjacent to a river. Floodplains stretch from the banks of a river channel to the base of the enclosing valley, and experience flooding during periods of high discharge.
- Infiltration ponds: A infiltration basin is used to manage storm water runoff, prevent flooding and downstream erosion, and improve water quality in an adjacent river, stream, lake or bay.

These results were shared with the local municipality and relevant stakeholders, and potentially included in the region's climate action plans.





The first two solutions from the EBA workshop were implemented in the HEC-RAS model to evaluate the results. Riparian reforestation was simulated changing the Manning's coefficient from the original 0.035 – in literature corresponding to “Fields and grasslands” – to 0.15 – corresponding to “Floodplains, trees” – in the most upstream riverbanks cross sections (from 46 to 134). Below are shown the results for RCP 4.5 2045-2095 TR200 respectively without and with the riparian reforestation implementation. Increasing Manning's coefficient makes the water flow slow down, and in a heavily urbanized area as Massa, this leads to a worsening of the flooded area.

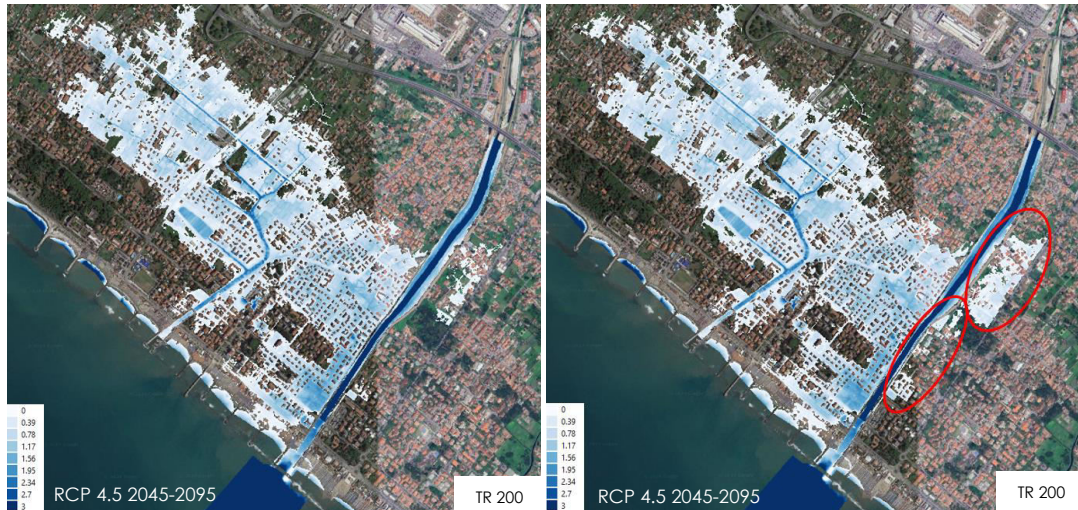


Figure 28. Hazard maps for river flood, return period 200 years, RCP 4.5 without and with riparian reforestation

Due to those preliminary results, it was necessary to implement the second EBA proposed: the floodplain enlargement. However, this solution is not practically feasible in such an urbanized area: it would be necessary to remove streets, buildings etc. due to the lack of space along the river area (see picture below).

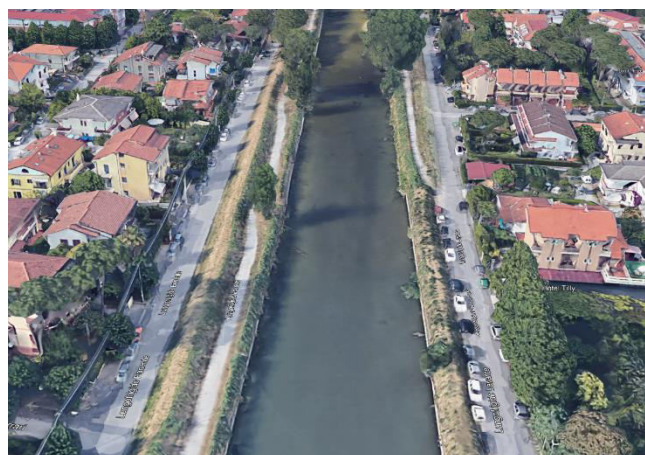


Figure 29. Urbanized area along river Frigido

So, instead of carrying out the mentioned above EBA, it was decided to implement a more realistic





solution that produce a similar effect: bed river excavation in the downstream riverbed (cross sections from 6 to 49). This was made by following a linear interpolation from the deepest point in cross section 6 to the deepest one in cross section 49.

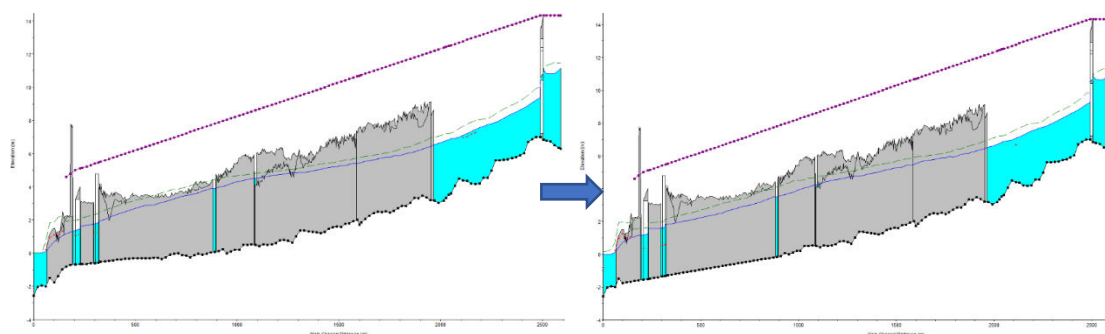


Figure 30. River Frigido profile – baseline and riverbed excavation.



Figure 31. Hazard maps for river flood, return period 100 years, RCP 8.5 without and with EBA implementation

The results show a good improvement in the flooded area extension for all the scenarios and return periods.

### 3.3 Vilanova i la Geltrú

Vilanova i la Geltrú is the capital city of Garraf comarca, in the province of Barcelona, Catalonia, Spain. The city has a growing population of approximately 66,000, and is situated 40 km south-west of Barcelona, with the coastal resort of Sitges some 10 km to the north-east. The environment of the city is remarkable for its natural values. The city is surrounded by a green/blue ring, formed by sea wetlands with the presence of protected species such as *Charadrius alexandrinus*. Vilanova i la Geltrú is a municipality located at 22 meters above mean sea level, though the higher part of the city is at 300 m above mean sea level. The main part of the population lives in the city center, but there are also several residential areas



spread in the city's territory.

Torrent de la Piera is the main river of the municipality. Totally located within the demarcation of la Geltrú, it collects the waters of the fondo de Santa Magdalena that descend from the corral de Carro and all those that descend from much of the foothills of migjorn del Montgrós. It flows to the beach of Sant Cristòfol, which has a length of 700 meters, an average width of about 100 meters and a total surface in sand of about 67,000 m<sup>2</sup>. In 2018 the naturalization work of the beach was completed, creating a dune system that prevents natural erosion.

Torrent de Sant Joan is the second river, formerly called the Ramusa stream. It has its head at the foot of the mountain range that goes from the Talaia to the Coll de les Palmeres and goes down between the Mas Ricart and the Mas Torrat.

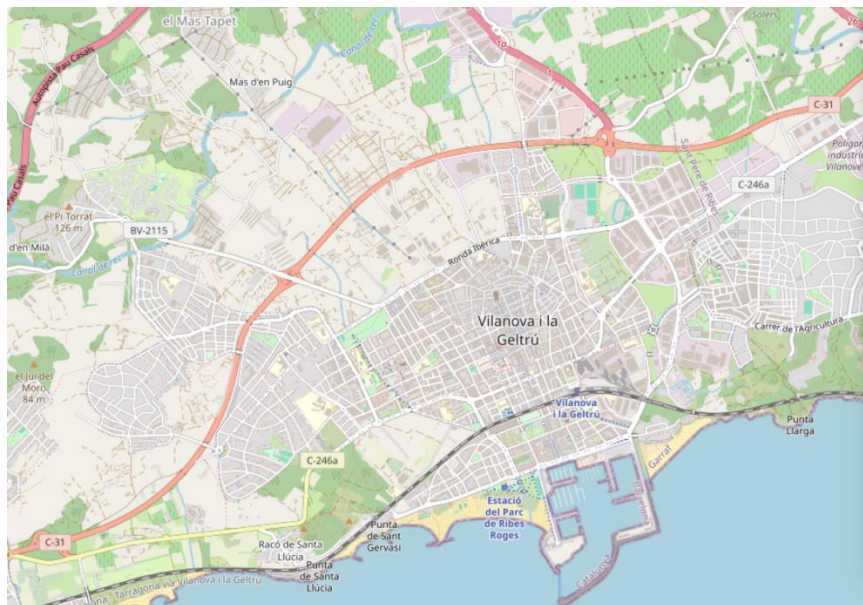


Figure 32. Vilanova i la Geltrú CCLL

As for Massa case study, a 1D/2D hydraulic model on HEC-RAS was implemented for Vilanova i la Geltrú. In this case, both Torrent de la Piera (on the right) and Torrent de Sant Joan (on the left) were modeled with a 1D structure. Riverbanks, levees, Manning's coefficient and bridges were defined. The minor river, torrent de Sant Joan, is hidden underground for about 500 meters.

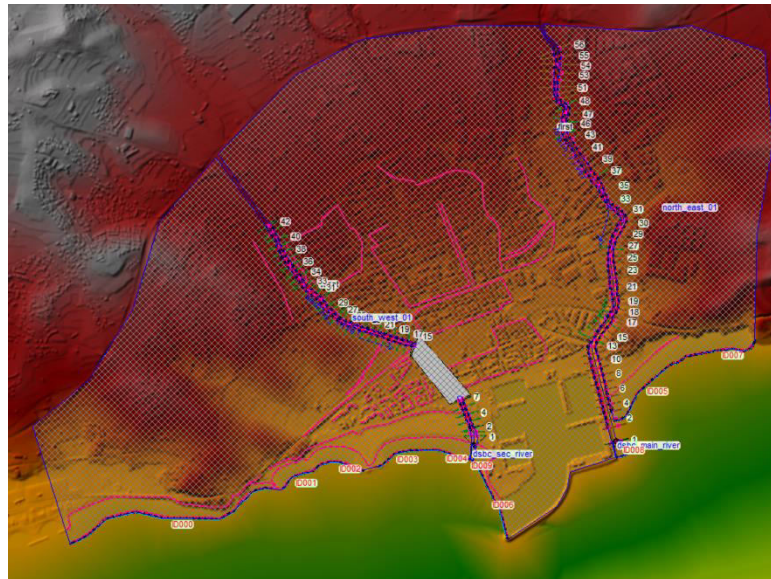


Figure 33. Study area in HEC-RAS

A DEM was added to the model, and the 2D Flow Areas were created with a mesh resolution of 10x10 meters (south-west) and 20x20 meters (north-east). Also, two 2D Flow Areas were added at the mouth of rivers in order to create the downstream boundary conditions needed. The lateral structures along the riverbanks are used to connect the 1D model with the 2D one. When the model's geometry has been completed, the hydrographs and boundary conditions are entered. The hydrographs for the different scenarios e return periods are provided by the previous hydrological model (LISFLOOD) and the extreme value analysis results. The initial flow of Torrent de la Piera corresponds to the minimum flow entered (20 m<sup>3</sup>/s) necessary to prevent it from drying out. For Torrent de Sant Joan this flow is 15 m<sup>3</sup>/s. The initial and boundary conditions on the coast are entered based on the previous model runs (SHYFEM, WWIII) and the extreme value analysis; they are the combination of data about storm surge, tide, wave runup and increase of relative mean sea level (only for projections).

As for Massa case, both river and coastal flood simulations were carried out, simulating a flood event from the two rivers while the sea level remains constant, and simulating an extreme sea flood event by fluctuating the water level, while the rivers maintain a constant flow.

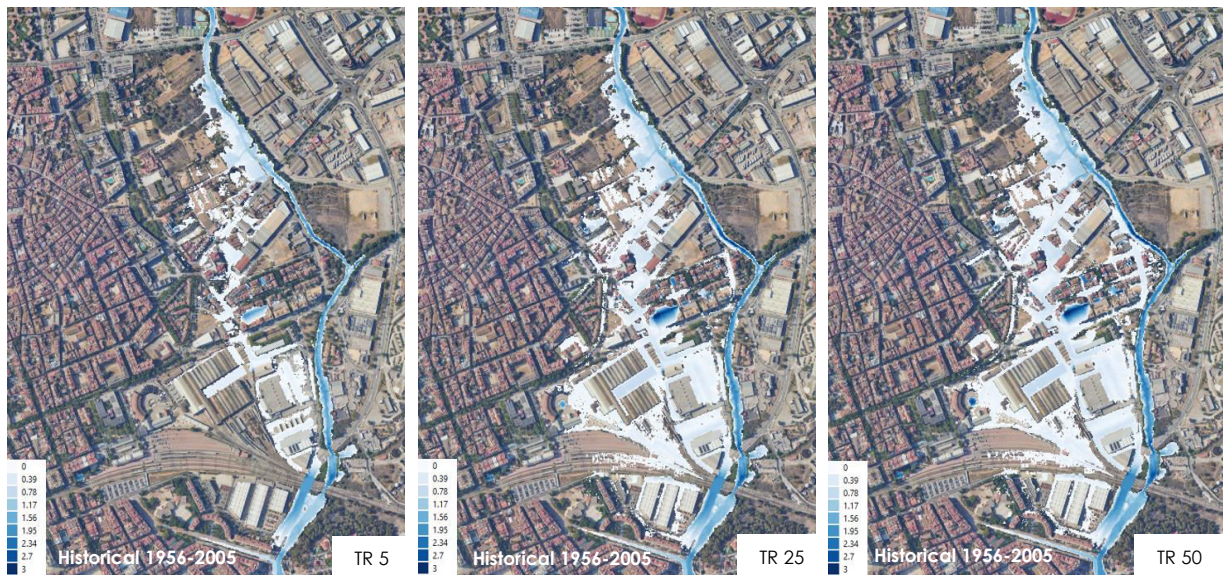
## RESULTS – RIVER FLOOD

The primary impact of river flood events is on the area near Torrent de la Piera, on the river's right side, so the results showed below are focused on that specific area. Although there are slight differences in the extent of the flooded areas, the main distinction between the scenarios lies in the depth of the water surface, which is higher in the more pessimistic future scenarios and it increases in the higher return periods.





Figure 34. Focus area in hazard maps



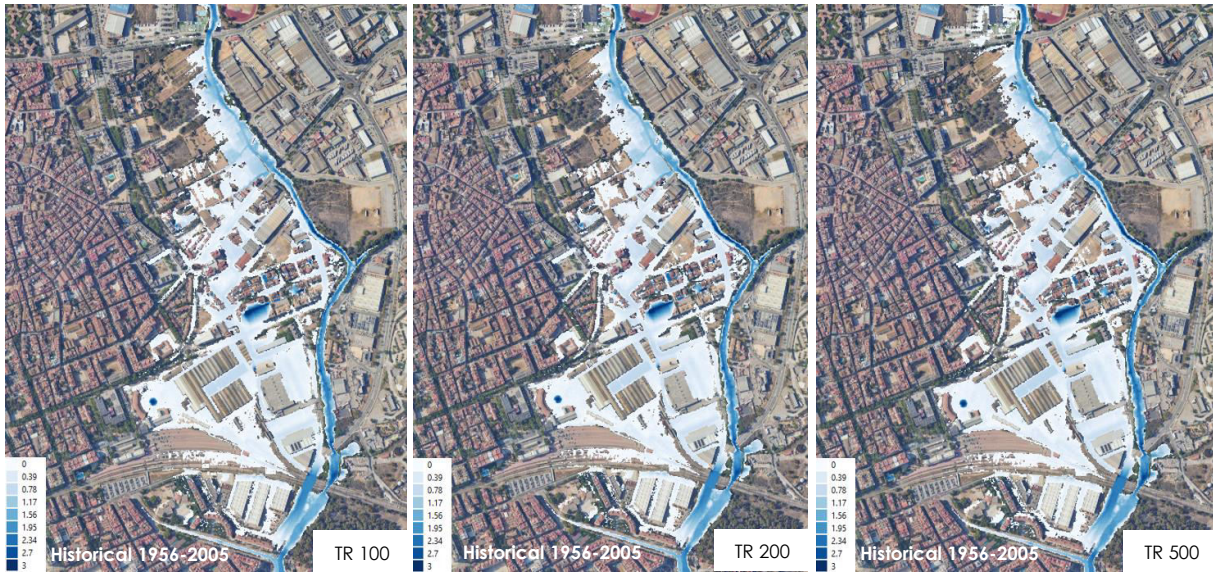


Figure 35. Hazard maps for river flood, return periods 5, 25, 50, 100, 200, 500 years, Historical 1956-2005

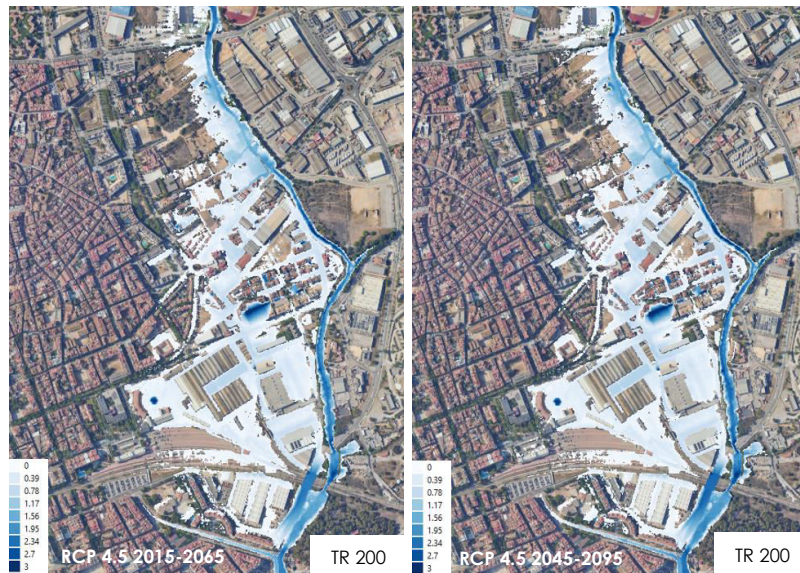


Figure 36. Hazard maps for river flood, return period 200 years, RCP 4.5



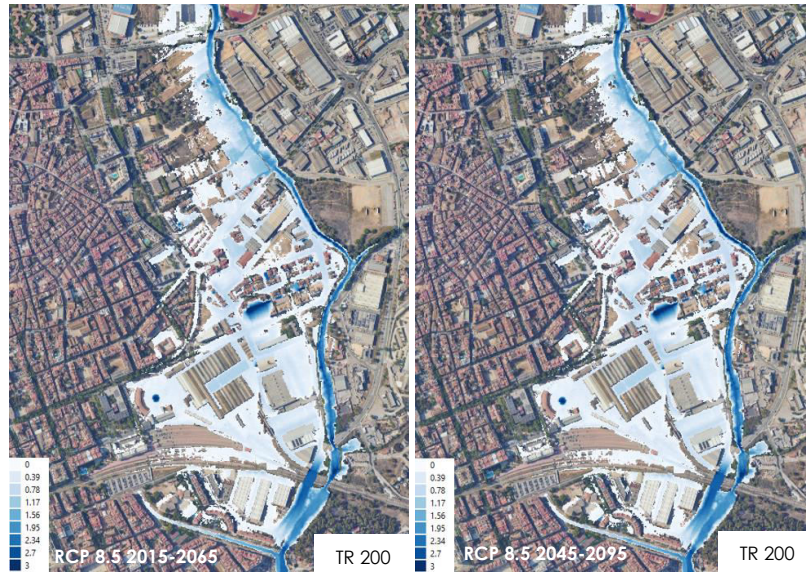


Figure 36. Hazard maps for river flood, return period 200 years, RCP 8.5

**RESULTS – COASTAL FLOOD**





Figure 37. Hazard maps for coastal flood, return period 500 years, Historical, RCP4.5, RCP 8.5

As for coastal events, the urban area is protected by a wall that separates the beach from the street next to it (see picture below). Even for the highest return period and the most pessimistic scenario, the city does not get flooded by sea extreme events, but the sandy beaches can be very affected, as the many activities that take place on them.



Figure 38. Wall between the beach and the street

## EBA

Ecosystem-based approaches (EBAs) have been implemented to reduce the impact of river floods. The work has been carried out in collaboration with Vilanova CCLL and WP7, who provided information about critical areas and ideas on how to reduce the impact. After a trial error process, the decisions were the following:

- Green overbanks elevation (2 m high, 60% slope, 3.5 m wide) in cross sections 45-38;
- Widen for 2 m on the right side cross sections 45-38;
- Widen for 2 m on the left side cross sections 36-32;
- Green overbanks elevation (2 m high, 60% slope, 3.5 m wide) in cross sections 13-19.



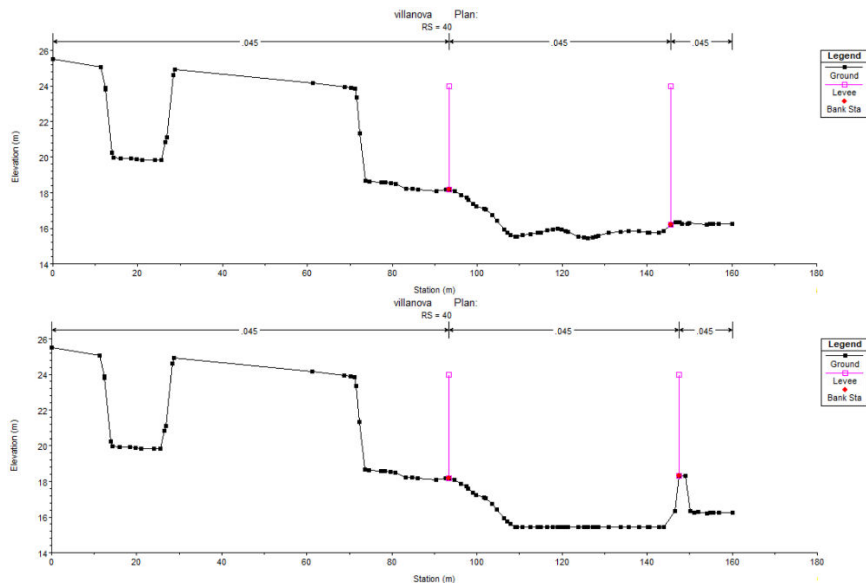


Figure 39. Before and after EBA implementation – Cross section 40

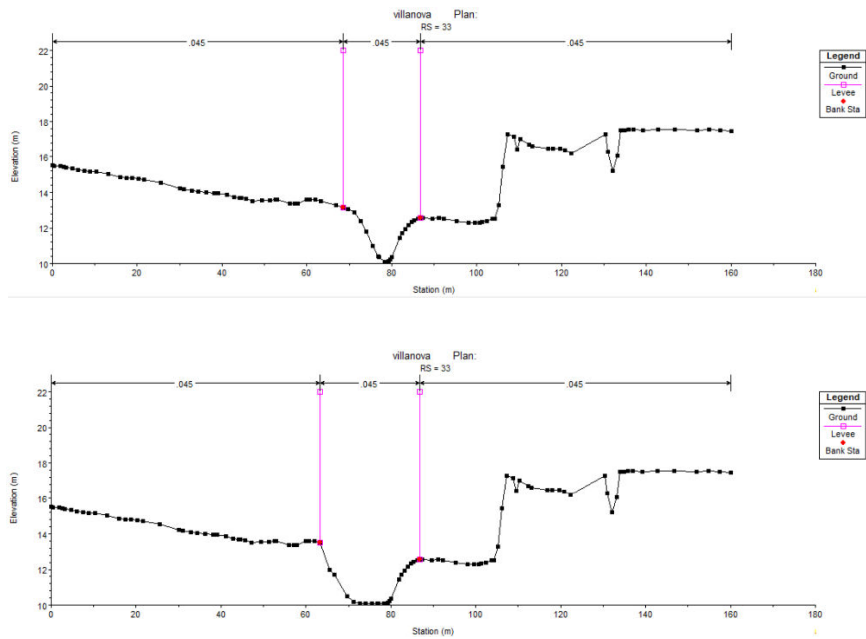
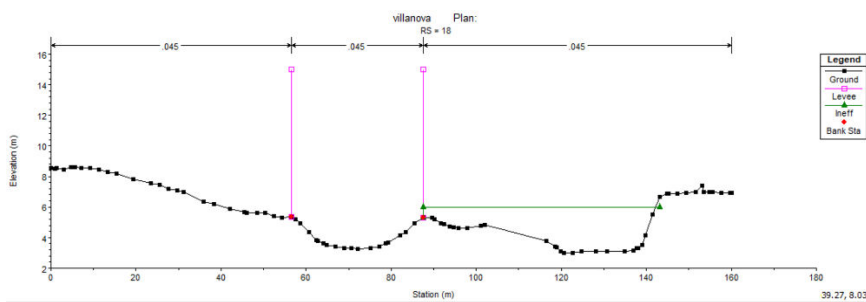


Figure 40. Before and after EBA implementation – Cross section 33



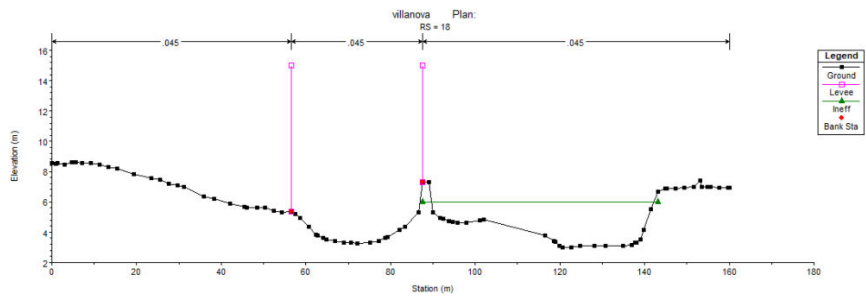


Figure 41. Before and after EBA implementation – Cross section 18

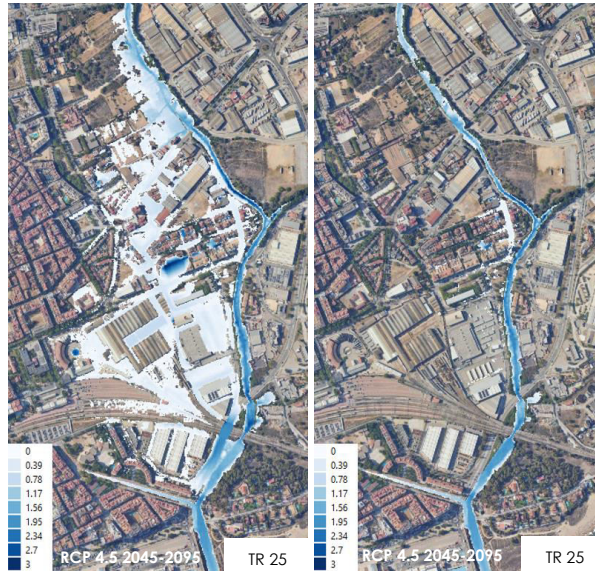


Figure 42. Hazard maps for river flood, return period 25 years, RCP 4.5 without and with EBA implementation

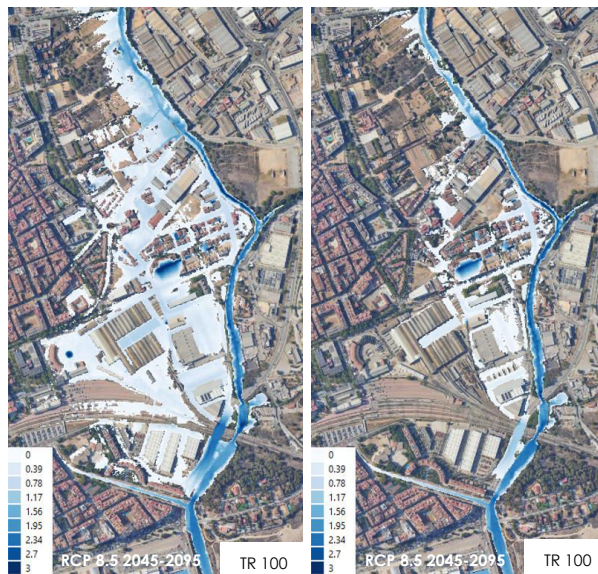


Figure 43. Hazard maps for river flood, return period 100 years, RCP 8.5 without and with EBA





## implementation

The results show a good improvement in the flooded area extension and water depth for all the scenarios and return periods.

### 3.4 Oarsoaldea

Oarsoaldea is a coastal county of the Basque Country, it is located in north-east of the province of Gipuzkoa, and is made up by four municipalities: Errenteria, Lezo, Oiartzun and Pasaia. The county has an area of 116.25 km<sup>2</sup> and about 72,000 inhabitants. Oarsoaldea is a geographically and geologically diverse area, from the sandstone flysch Cliffs of Jaizkibel, which protect the Pasaia Bay, to the granite peaks of Aiako Harria, ascending through the beech and oak groves of the Natural Park of the same name, like the Oiartzun River basin. Among this sandstone and granite mountain areas is located a natural corridor connecting the Iberian Peninsula and Europe, which is now the most urbanized area of the county.

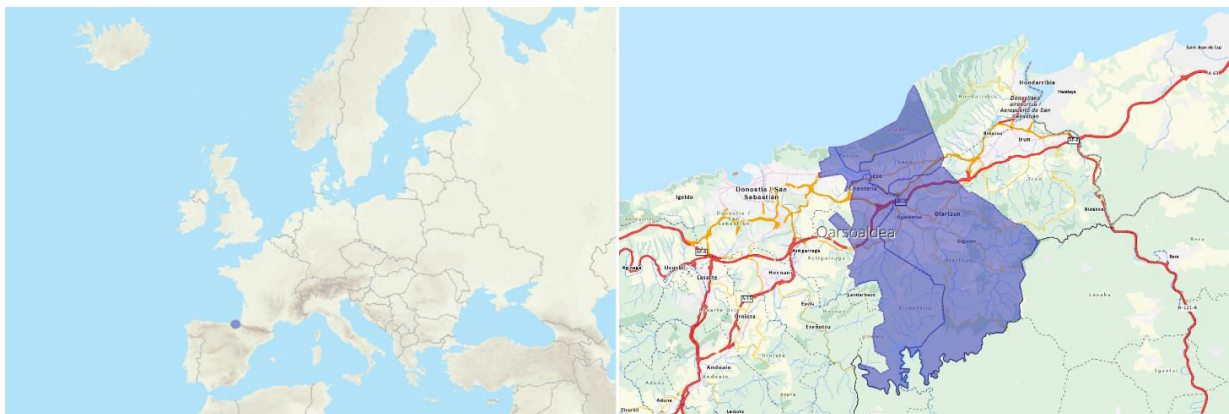


Figure 44. Oarsoaldea CCLL

The main river of the case study area is Oiartzun, which rises in the Aiako Harria massif at an altitude higher than 700 m and flows into the Bay of Biscay (Atlantic basin) at the Bay of Pasaia after 18.5 km. The second river modeled is Lintzirin which is hidden underground for most of its length, and it joins the Oiartzun river in Parque por la Paz.

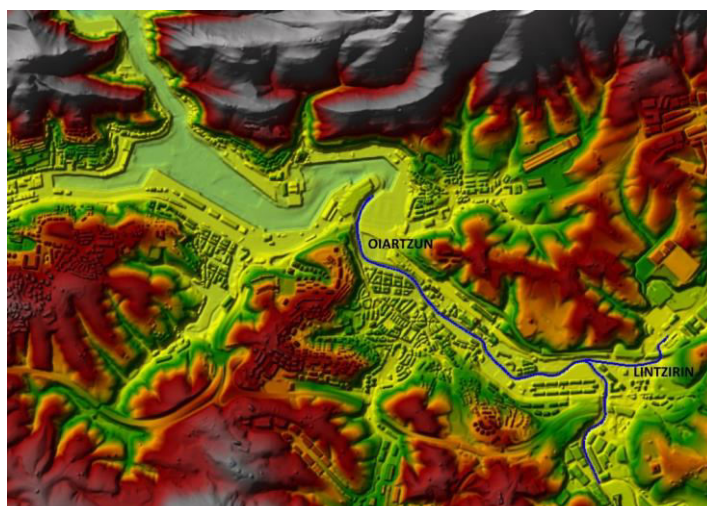




Figure 45. Oarsoaldea DEM in HEC-RAS

A 1D/2D hydraulic model on HEC-RAS was implemented, where both rivers have a 1D structure.

A DEM with buildings was included in the model, but the information about the bathymetry of Pasaia Bay where missing, in fact a different DEM with the bathymetry of the bay area was then added. These two DEM have a different zero reference: the inland DEM altimetry is referred to the geoid model EGM08\_RED NAP, which is +2.172 m above the zero level of the bathymetry DEM. Moreover, the long-term average value of the water level with respect to the zero of the bathymetry inside the bay is +2.57 m (based on the analysis of the period 2007-2022). Since for the urban scale flood model the important data is the water level with respect to the inland DEM, a value of 0.398 m is calculated to be the zero of the mean sea level.

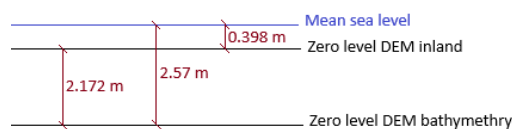


Figure 46. Zero level reference of DEMs and mean sea level

The 2D Flow Area is modeled with two meshes with a mean resolution of 20x20 meters that increases up to 5x5 meters near some 2D area breaklines. The Breaklines layer is a set of polylines used to enforce cell faces along linear features, such as high ground, to direct the movement of water through the 2D domain and it is used to have more accuracy in the 2D hazard maps.

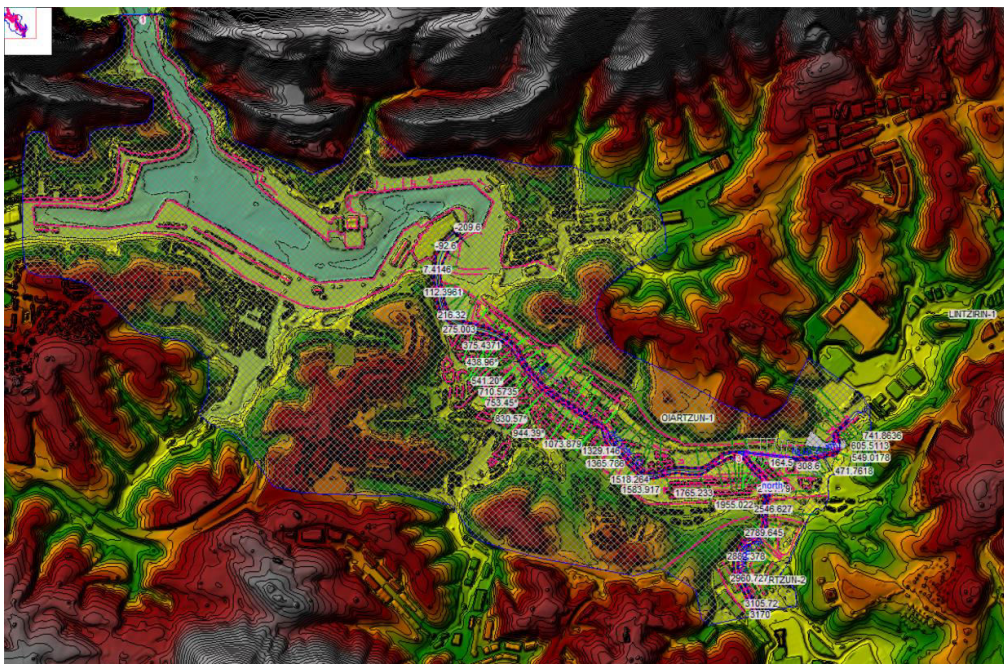




Figure 47. Study area in HEC-RAS with DEM, 2D Flow Areas, Cross-sections

As for the previous case studies, both river and coastal flood were simulated. The first one uses hydrographs from the hydrological model (LISFLOOD) and the extreme value analysis as input, while the sea level remains constant. Coastal flood simulations use data from SHYFEM and WWIII to run the effects of tides, which are very high in the Basque country (more than 2 m), storm surges and relative mean sea level rise (for future scenarios only). Wave runup is not take into account given the geographical conformation of the area (port bay without beaches).

## RESULTS – RIVER FLOOD

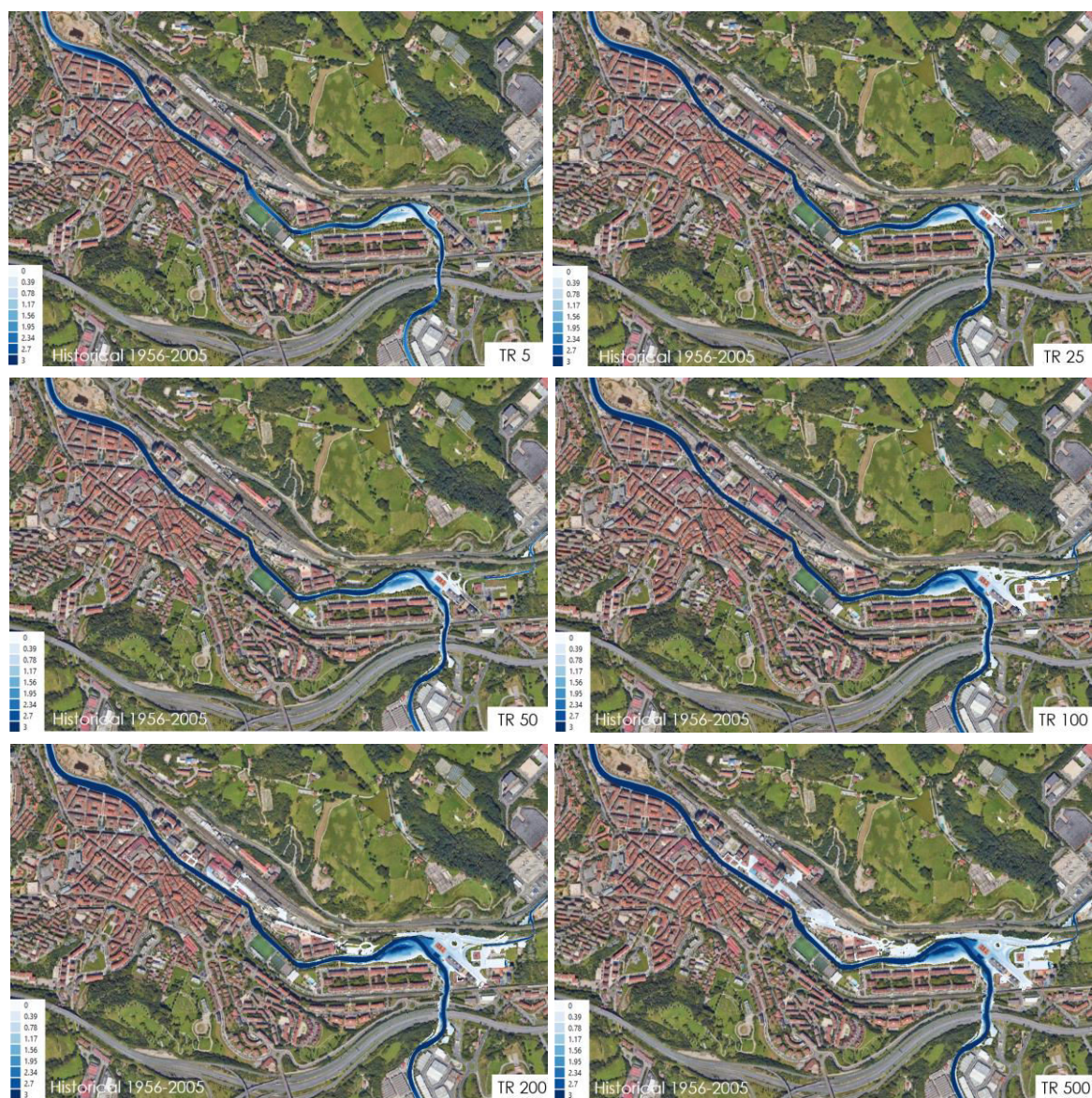


Figure 48. Hazard maps for river flood, return periods 5, 25, 50, 100, 200, 500 years, Historical 1956-2005





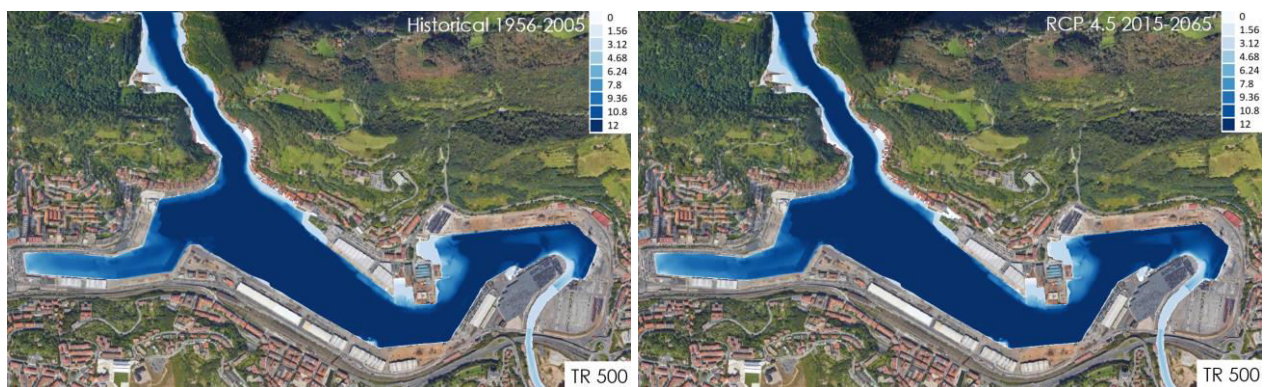
Figure 49. Hazard maps for river flood, return period 200 years, RCP 4.5



Figure 50. Hazard maps for river flood, return period 200 years, RCP 8.5

The results of hydrological model and extreme value analysis show that the future scenarios are associated with higher flow rates than the historical, but unlike the other case studies, the RCP 4.5 scenario corresponds to higher flow rates than the 8.5 scenario. For this reason, the flooded area in RCP 4.5 is more extended than in RCP 8.5.

## RESULTS – COASTAL FLOOD



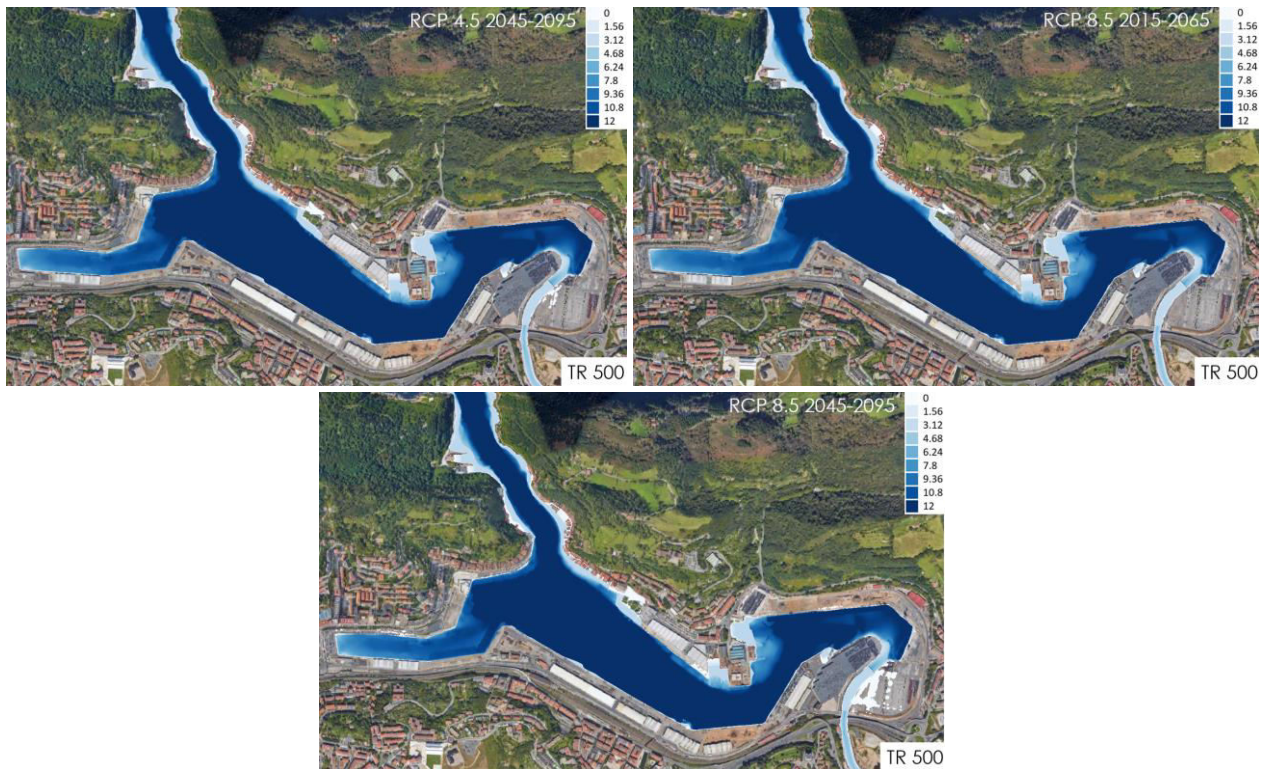


Figure 51. Hazard maps for coastal flood, return period 500 years, Historical, RCP4.5, RCP 8.5

The results from SHYFEM show that water level due to storm surges will decrease in the future. Nevertheless, relative mean sea level will rise so that the sum of the two contributions will be higher in future scenarios. The urban scale flood model shows that, even for the highest return period, the city is barely affected by coastal flood events. Only the northern and the eastern area of the bay are flooded due to the sea in the worst cases. The reason is that the area is subject to very intense tidal excursions, so the port is built about 4 meters above mean sea level to be protected from the water level.

### EBA

Before the SCORE project, several nature-based adaptation measures have been taken in the municipalities of Oarsoaldea. One of them is the realization of Parque de la Paz, a fluvial park that takes place exactly where Lintzirin river joins Oiartzun. The fluvial park has a surface area of about 42000 m<sup>2</sup> and it creates lots of benefit to the city, as flood risk reduction, reduction of damage costs and ecosystem services like carbon storage and recreational services.





Figure 52. Fluvial park in Oarsoaldea

The EBA chosen to be modelled consists on measuring the effect of the existing EBA, the fluvial park, to calculate the flood damage avoided by the presence of the park that exists nowadays, compared to what would occur if it were a built-up area. So, a reverse EBA exercise has been carried out: modelling what it would be like if the EBA did not exist and the park was a built-up area.

To implement this kind of reverse EBA, it was necessary not to let water overflow in the park, elevating the lateral structures and the DEM in that area.



Figure 53. Hazard maps for river flood, return period 5 years, RCP 4.5 without and with EBA implementation

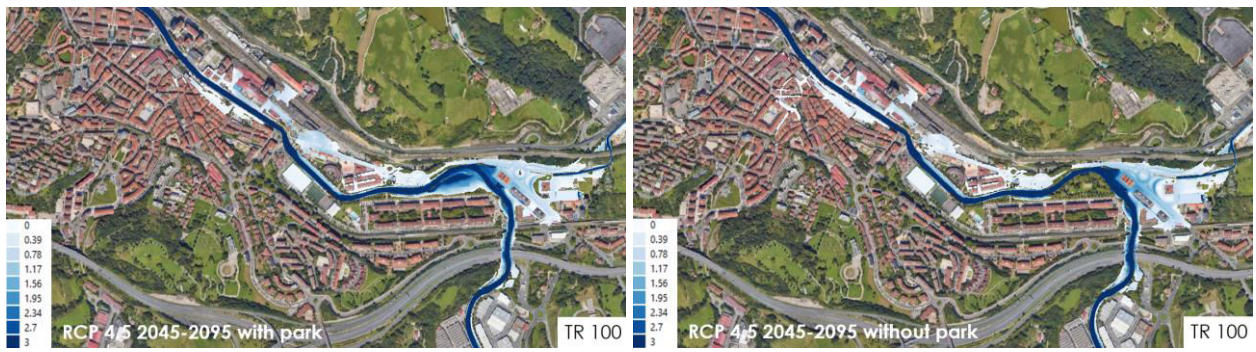


Figure 53. Hazard maps for river flood, return period 100 years, RCP 4.5 without and with EBA implementation

The results show that if the park doesn't flood, then the flood spreads more in the urban area, especially in the east side and in the city centre for higher return period.

The difference between the two scenarios is not so obvious because the fluvial park floods even for low return periods meaning low flow rates. This means that, for higher return periods, the park is already full of water before hydraulic peak arrives, so the park can no longer contain water that spreads elsewhere.



## 4 CONCLUSIONS

This report presents the application package of short-term hazard modelling developed for the WP3's four frontrunner CCLLs: Samsun, Massa, Vilanova i la Geltrú, and Oarsoaldea. Two types of modelling for these cities were considered in this task at an urban scale: land flood modelling and coastal flood modelling. This report may serve as an informative guide for the use of tools included in the package of short-term hazard modelling presented in D3.7. While the flood modelling methodologies applied in the four frontrunner cities are fundamentally the same, there are differences in the application due to various factors such as urbanization characteristics on one hand and the availability of sufficient and qualified data on the other hand. Therefore, the modelling stages and results for each city are presented as separate case studies.

It is important to highlight that the application of methods for flood mapping as a consequence of various climate forcings (from the historical to future scenarios) shows that for some cities (e.g., Massa), the future impact of coastal flooding could become comparable to that of hydrological flooding. For all the cities, the extent of the flooding areas shows an increasing trend not only for longer return periods but also based on the climate scenario used (from historical, to RCP4.5, to RCP8.5), and even for longer timeframes (i.e., with more intense events predicted when extending the projection scenario beyond 2050).

The short-term hazard modelling package carried out in Task 3.4 and described in this document represents a key milestone in SCORE's WP3 activities, as these will be used to directly inform the flood modelling that will be carried out in the context of Task 3.4. Specifically, these modelling components, together with the exposure and vulnerability assessments carried out in WP6, will allow for the computation of metrics related to economic losses for low-probability events across various scenarios.

Additionally, the results can be used, both for verification and intercalibration purposes, in the development of Digital Twins (WP8). This will also contribute to the realization of Early Warning Support Systems (EWSS) services. The models used have proven to be particularly suitable for evaluating the implementation of Ecosystem-based Approaches (EBAs), which have been discussed in participatory sessions with the partners of the CCLLs in Massa, Vilanova i la Geltrú, and Oarsoaldea, within the activities of WP7.





## 5 REFERENCES

- Beden, N., & Ülke Keskin, A. (2021). Flood map production and evaluation of flood risks in situations of insufficient flow data. *Natural hazards*, 105(3), 2381-2408.
- Beden, N., Demir, V., & Ülke Keskin, A. (2020). Trend Analysis of SPI and PNI Drought Indices in Samsun City. *Dokuz Eylül University Faculty of Engineering Science and Engineering Journal*, 22(64), 107-116. <https://doi.org/10.21205/deufmd.2020226411>
- Brandini, C., Ortolani, A., Bondoni, M., Beden, N., Demir, V., Efe, B., ... & Oksal, S. A. S. D3. 7: Package of short-term hazard modelling.
- Brunner, G. W. (2016). HEC-RAS river analysis system: hydraulic reference manual, version 5.0. *US Army Corps of Engineers—Hydrologic Engineering Center*, 547.
- Demir, V., & Kisi, O. (2016). Flood hazard mapping by using geographic information system and hydraulic model: Mert River, Samsun, Türkiye. *Advances in Meteorology*, 2016.
- Demir, V., & Keskin, A. U. (2019). Determination of Manning roughness coefficient by Cowan method and Remote Sensing. *Gazi journal of engineering sciences*, 5(2), 167-177..
- Demir, V., & Keskin, A. Ü. (2020). Obtaining the Manning roughness with terrestrial-remote sensing technique and flood modelling using FLO-2D: A case study Samsun from Türkiye. *Geofizika*, 37(2), 131-156.
- Demir, V., Beden, N. Ülke, A. (2021). Review and Comparison of Flood Modelling Methods. *Eur. J. Sci. Technol.* 2021, 1013–1021, doi:10.31590/ejosat.1010220.
- Floods Directive, (2018), “: Floods Directive Reporting Guidance 2018” [https://cdr.eionet.europa.eu/help/Floods/Floods2018/GuidanceDocuments/FD\\_ReportingGuidance.pdf](https://cdr.eionet.europa.eu/help/Floods/Floods2018/GuidanceDocuments/FD_ReportingGuidance.pdf)
- Korkmaz, B., & Efe, B. (2021). Trend Analysis of Samsun and Bafra Rainfall Data. *European Journal of Science and Technology*(23), 844-850. <https://doi.org/10.31590/ejosat.883770>
- Lea, D., Yeonsu, K., Hyunuk, A. (2019). Case Study of HEC-RAS 1D-2D Coupling Simulation: 2002 Baeksan Flood Event in Korea. *Water (Switzerland)* 2019, 11, 1–14, doi:10.3390/w11102048.
- MGM (2024), Turkish State Meteorological Service, <https://www.mgm.gov.tr/veridegerlendirme/il-ve-ilceler-istatistik.aspx?k=undefined&m=SAMSUN>, access date: 28.05.2024
- Papaioannou, G.; Efstratiadis, A.; Vasiliades, L.; Loukas, A.; Papalexiou, S.M.; Koukouvinos, A.; Tsoukalas, I.; Kossieris, P. (2018) An Operational Method for Flood Directive Implementation in Ungauged Urban Areas. *Hydrology*, 5, 1–23, doi:10.3390/hydrology5020024.
- Rebollido E L, Iglesias G , (2023) D1.4 - Report of baseline risk analysis
- Rebollido E L, Iglesias G , (2022) D1.2-Map and report of key climate-change hazards
- Rebollido E L, Rodríguez J G I, (2021) D1.1 Package of -Literature Review Report.
- Roelvink, D.; Reniers, A.; van Dongeren, A.; de Vries, J.V.T.; McCall, R.; Lescinski, J. Modelling storm impacts on beaches, dunes and barrier islands. *Coast. Eng.* 2009, 56, 1133–1152.
- Şen Z (2009). Flood disaster and modern calculation methods. Water Foundation Publications. 252p.
- Ülke Keskin, A., Kir, G., & Zeybekoğlu, U. (2023). Evaluation of The Homogeneity and Trends of Precipitation, Temperature and Wind Speed Parameters in The Black Sea Region . *Sustainable Engineering Practices and Technological Developments Magazine*, 6(1), 129-145. <https://doi.org/10.51764/smutgd.1260628>
- USACE, 2018 (U.S. Army Corps of Engineering) HEC-RAS 5.0 Supplemental to User’s Manual; U.S. Army Corps of Engineering: Huntsville, AL, USA, 2018.

